



저작자표시-비영리-변경금지 2.0 대한민국

이용자는 아래의 조건을 따르는 경우에 한하여 자유롭게

- 이 저작물을 복제, 배포, 전송, 전시, 공연 및 방송할 수 있습니다.

다음과 같은 조건을 따라야 합니다:



저작자표시. 귀하는 원저작자를 표시하여야 합니다.



비영리. 귀하는 이 저작물을 영리 목적으로 이용할 수 없습니다.



변경금지. 귀하는 이 저작물을 개작, 변형 또는 가공할 수 없습니다.

- 귀하는, 이 저작물의 재이용이나 배포의 경우, 이 저작물에 적용된 이용허락조건을 명확하게 나타내어야 합니다.
- 저작권자로부터 별도의 허가를 받으면 이러한 조건들은 적용되지 않습니다.

저작권법에 따른 이용자의 권리는 위의 내용에 의하여 영향을 받지 않습니다.

이것은 [이용허락규약\(Legal Code\)](#)을 이해하기 쉽게 요약한 것입니다.

[Disclaimer](#)

A Thesis
For the Degree of Master in Veterinary Medicine

**Protective Effects of an Acidic
Polysaccharide of *Panax ginseng* on
Radiation-induced Hematopoietic and
Gastrointestinal Injury in Mice**

Department of Veterinary Medicine

GRADUATE SCHOOL
JEJU NATIONAL UNIVERSITY

Dae Seung Kim

2016. 8

**Protective Effects of an Acidic Polysaccharide of
Panax ginseng on Radiation-induced Hematopoietic
and Gastrointestinal Injury in Mice**

Dae Seung Kim
(Supervised by professor Youngheun Jee)

A thesis submitted in partial fulfillment of the requirement
for the degree of Master in Veterinary Medicine

2016. 06.

This thesis has been examined and approved by

.....
Thesis director, Yoonkyu Lim, Veterinary Medicine, Jeju National University

.....
Ginnae Ahn, Marine Bio Food Science, Chonnam National University

.....
Youngheun Jee, Veterinary Medicine, Jeju National University

Department of Veterinary Medicine
GRADUATE SCHOOL
JEJU NATIONAL UNIVERSITY

CONTENTS

Contents	1
List of tables	2
List of figures	3
List of abbreviations	4
Abstract	6
Introduction	7
Materials and methods	10
Results	15
Discussion	21
References	25
Tables	30
Figures	32
Abstract in Korean	51

LIST OF TABLES

Table 1. Immunohistochemical localization of different antibodies in the small intestine of mice.

Table 2. The effect of APG on survival rates after 9 Gy γ -ray irradiated.

LIST OF FIGURES

- Figure 1.** The effect of APG on endogenous splenocyte colonies from irradiated mice.
- Figure 2.** Comet assay of APG effect on irradiation-induced DNA damage in splenocytes comparing.
- Figure 3.** The effect of APG on apoptosis of splenocytes using DAPI staining.
- Figure 4.** The effect of APG extract on proliferation of splenocytes.
- Figure 5.** Representative images showing the apoptotic cells in the intestinal sections with H&E and TUNNEL assay.
- Figure 6.** p53 immunoreactivity in small intestines of mice 24h after γ -ray irradiation.
- Figure 7.** Bax immunoreactivity in small intestines of mice 24h after γ -ray irradiation.
- Figure 8.** Bcl-2 immunoreactivity in small intestines of mice 24h after γ -ray irradiation.
- Figure 9.** Bcl-X_{SL} immunoreactivity in small intestines of mice 24h after γ -ray irradiation.
- Figure 10.** Cytochrome C immunoreactivity in small intestines of mice 24h after γ -ray irradiation.
- Figure 11.** Cleaved Caspase-3 immunoreactivity in small intestines of mice 24h after γ -ray irradiation.

LIST OF ABBREVIATIONS

APG	Acidic polysaccharide of <i>Panax ginseng</i>
Con A	Concanavalin A
CFUs	Colony forming units
DAB	3,3'-diaminbenzidine tetrachloride
DAPI	4'6-diamidino-2-phenylindole dihydrochloride
FBS	Fetal bovine serum
FDA	Federal drug administration
GI	Gastrointestinal
GM-CSF	Granulocyte-macrophage colony stimulating factor
GPx	Glutathione peroxidase
H&E	Hematoxylin and eosin
IFN	Interferon
IL	Interleukin
i.p.	Intraperitoneal injection
IR	Ionizing radiation
PBS	Phosphate-buffered saline
ROS	Reactive oxygen species
SOD	Superoxide dismutase

TNF	Tumor necrosis factor
TUNEL	Terminal deoxynucleotidyl transferase mediated dUTP Nick End Labeling
WBI	Whole-body irradiation

1. ABSTRACT

An acidic polysaccharide of *Panax ginseng* (APG), so called Ginsan, is known to have important immunomodulatory activities. It was recently reported that APG had radioprotective effects in mice but the detailed mechanism was not fully elucidated. We investigated the potential of APG to protect the hematopoietic and gastrointestinal of mice from radiation injury by a single whole-body irradiation (WBI) *in vivo*. From our results, the counts of endogenous colony forming units (CFUs) increased in APG-treated mice, indicating that APG induced the regeneration of hematopoietic cells. In splenocytes, APG treatment decreased the percent of tail DNA, a parameter of DNA damage, and also accelerated the proliferation and recovery of splenocytes, compared with untreated, irradiated controls. Furthermore, the number of apoptotic cells was significantly decreased in splenocytes of APG-treated mice compared with that of irradiated controls. Also, APG treatment caused the lengthening of villi and a numerical increase of crypt cells in the small intestine at 3.5 days after 7 Gy irradiation compared to irradiated, non-treated controls. In addition, the expression levels of apoptosis-related molecules in the jejunum were investigated using immunohistochemistry. As a result, it increased the expression levels of anti-apoptotic proteins (Bcl-2 and Bcl-X_{S/L}) and dramatically reduced the expression levels of pro-apoptotic proteins (p53, BAX, cytochrome C and Caspase-3). Overall, this study shows that APG can enhance the regeneration of hematopoietic stem cells, and promote the repair of damaged cells or the proliferation of the immune cells. Therefore, our current data provide evidence that APG might be a useful adjunct to therapeutic irradiation as a protective agent for the gastrointestinal tract of cancer patients.

Key words : Acidic polysaccharide of *Panax ginseng*, Ionizing radiation, Apoptosis, Radioprotection

2. INTRODUCTION

Radiation is the treatment of choice for a majority of cancer patients. Although such irradiation is directed at malignant tissue, the surrounding normal tissues are also affected (Weiss. 1997; Mashiba et al. 1979; Bogo et al. 1985; Satoh et al. 1982). The major detrimental effect of ionizing radiation (IR) on normal tissue cells is the induction of oxidative stress, the disturbance in the equilibrium status of pro-oxidant and antioxidant systems in favor of pro-oxidation *in vivo* (Lee et al. 2009). In addition, oxidative stress induced by exposures to IR causes radiolysis of water in the cell, generating collectively reactive oxygen species (ROS) such as hydrogen peroxide, hydroxyl radical, and super oxide anion (Lee et al. 2009). The produced ROS attacks diverse cellular macromolecules such as DNA, lipids, and proteins and induces cell death including apoptosis *in vitro* or *in vivo* (Lee et al. 2009; Kim and kim. 2010; Park et al. 2010). In particular, the exposure to IR leads to the destruction of the lymphoid and hemopoietic systems by increasing apoptosis of not only proliferating stem cells such as jejunal crypt cells, but also radiosensitive lymphocytes causing ROS production in animals (Andreson and Warner. 1976).

IR-induced hematopoietic failure was the primary cause of death after exposure to a moderate or high dose of total body irradiation. Hematopoietic stem cells are highly sensitive to IR as well as chemotherapeutic drugs administered to cancer patients. In fact, myelosuppression and hematopoietic dysfunction are the most common clinical complications of these treatments (Chen et al. 2007). Immediately after irradiation, intestinal crypt cells undergo apoptosis, and intestinal stem cells cannot differentiate quickly enough to repopulate the villi. The result is a diminution and blunting of the height of villi and subsequent functional incapacity including malabsorption, gastrointestinal (GI) bleeding and fatal destruction of GI tissue, commonly known as the GI syndrome (Chen et al. 2007). Thus, identifying effective and useful substances for the prevention or rescue of GI injury from radiation

exposure is very important. However, no effective medication has yet been found for the treatment of defense from radiation-induced GI injury. Due to these reasons, although IR is a useful tool in a wide variety of fields such as industry, agriculture, military operations, and medicinal researches, especially for cancer therapies, their practical applicability has been limited for many years (Moon et al. 2008; Moulder. 2002, 2003; Pellmar and Rockwell. 2005). Efforts to develop effective agents to alleviate the harmful effects of IR have mounted correspondingly. This has been all the more prompted by the scarcity of products approved by Federal Drug Administration (FDA) (Park et al. 2010). The majority of radioprotectors under active investigation are designed to scavenge IR induced intracellular free radicals and inhibit apoptosis, averting initial cascades of radiochemical events in cells following IR exposure (Stone et al. 2004; Park et al. 2008a, b, 2010). In particular, various natural products with antioxidant and cyto-protective resources have begun to receive attention as possible radiation modifiers (Park et al. 2008a-c). Previous studies have reported that various natural products i.e. *Elaeocarpus sylvestris*, *Peaonia japonica* and *Ecklonia cava* induce the radioprotective effects as improving lymphoid or hemopoietic systems via decreasing apoptosis as well as ROS production (Park et al. 2008a-c). Considering the fact that most of the potent agents under study are experimental, the repertoire of putative natural product radioprotective agents needs further expansion, by incorporating more locally abundant materials.

Ginseng, the root of *Panax ginseng* C.A. Meyer, is well-known and widely used in traditional Oriental medicine. Its compounds include water-soluble factors, polysaccharides, proteins and saponins (Kim et al. 2007). A soluble acidic polysaccharide extracted from *Panax ginseng* (APG), ginsan, has proved to be a stimulant that causes normal lymphoid cells to proliferate and to Produce cytokines such as interleukin (IL)-1, IL-2, interferon (IFN)- γ and tumor necrosis factor (TNF)- α (Shin et al. 2002). APG treatment protects mice from the lethal effects of IR, and enhances the number of hematopoietic and immune cells such as bone marrow cells

and spleen cells by inducing a variety of hematopoietic growth factors such as IL-1, IL-6, IL-12, TNF- α and granulocyte-macrophage colony stimulating factor (GM-CSF) (Song et al. 2003). In addition, APG modulates the radiation-induced disturbance of antioxidant enzymes such as superoxide dismutase (SOD), catalase and glutathione peroxidase (GPx) (Han et al. 2005). So far, the radioprotective effect of APG has been attributed to its immunomodulatory activity. In this study, we studied the ability of APG to offset damage to the hematopoietic and gastrointestinal injury of mice subjected to a whole-body irradiation (WBI).

3. MATERIALS AND METHODS

Mice

C57BL/6 female mice were purchased from Orientbio Inc. (Sungnam, Korea) were used for the experiment at the age of 6 to 8 weeks old about 20-25 g body weight. According to the guiding principle for the Care and Use of Laboratory Animals of the Institutional Ethical Committee, experimental mice were housed in conventional animal facilities with a NIH-07 approved diet and water supplied ad libitum at a constant temperature (23 ± 1 °C). All mice were randomly separated into three groups i.e. non-irradiated (Non IR), irradiated control group (IR) and APG plus irradiated group (IR + APG).

Preparation and treatment of APG compound

As described in our previous report (Hwang et al. 2011), APG was obtained from Dr. Jie-Young Song (Korea Cancer Center Hospital, Seoul, Korea) (Song et al. 2002). APG dissolved in phosphate-buffered saline (PBS) (pH 7.4) was injected intraperitoneally twice into mice with 10 mg/kg b.w. dose first at 18 h and then again at 2 h before irradiation. Additional two groups of mice, non-irradiated mice and irradiated control mice injected i.p. with PBS, were treated as controls.

Irradiation with ^{60}Co γ -rays

Each mouse was placed in a separate plastic container (3×3×11 cm) and given a single dose of WBI at dose rate of 1.5 Gy / min at a source-surface distance of 150 cm from a ^{60}Co irradiator (Theratron-780 teletherapy unit, Applied Radiological Science Institute, Jeju National University).

Animal survival

To determine the radioprotective capacity of APG compound, animals from two experimental groups, irradiated control group (n = 21) and APG plus irradiated group (n = 13), were monitored daily for survival until 30 days after exposure to 9 Gy of γ - ray irradiation. Surviving mice were euthanized by cervical dislocation at 31 days after WBI.

Endogenous hematopoietic colony forming units (CFUs) assay

To confirm the ability of APG to rescue and repopulate hematopoietic stem cells in irradiated mice, we examined the spleens to calculate endogenous colony forming units (CFUs). Spleens were removed from the mice (n = 8/group), and their surfaces were examined with the naked eye to score for macroscopic colonies at 9 days after exposure to 7 Gy of irradiation (Park et al. 2008).

Alkaline comet assay

To determine the cytoprotective effects of APG on oxidative DNA damages induced in peripheral blood lymphocytes, alkaline comet assay was used. At 1 day after exposure to 2 Gy of IR, peripheral blood lymphocytes isolated from mice of each group (n = 6/group) were used for this assay. The cells were lysed in lysis buffer (2.5 M NaCl, 100 mM Na₂-EDTA, 10 mM Tris, and 1% Triton X-100, pH 10) for 1h at 4 °C. After electrophoresis, the DNAs were observed under a fluorescence microscope and analyzed by using the Komet 5.5 program (Kinetic Imaging, Liverpool, UK). The percentage of fluorescence in the tail DNAs (%), tail lengths (μ m) of 100 cells per slide were recorded.

4'6-diamidino-2-phenylindole, dihydrochloride (DAPI) staining

To confirm the cytoprotective effect of APG on the radiation-induced apoptosis of peripheral blood lymphocytes, DAPI staining was performed. The lymphocytes were suspended in RPMI-1640 medium supplemented with 10% FBS and 1% antibiotics. The lymphocyte suspensions (containing 1×10^6 cells) were then washed with PBS and fixed in Carnoy's fixative solution. The cells were stained with 1 mg/ml of DAPI solution (Sigma-Aldrich) for 10 min in a dark room. Morphological changes of apoptotic cells, such as apoptotic body formation with fragmented nuclei and chromatin condensation, were viewed in a fluorescence microscope (Leica, Wetzler, Germany). The frequency of apoptotic cells was calculated as the ratio of apoptotic cells detected to total lymphocytes (400-500 cells in each mouse) inspected.

³H-thymidine incorporation assay

To assess whether APG stimulated the regeneration and proliferation of splenocytes damaged by irradiation, a thymidine incorporation assay was performed. The splenocytes were isolated 3, 9, 13 days after exposure to 2 Gy of irradiation and seeded at 4×10^5 cells/well in 96-well round-bottom microtiter plates (Nunc, Copenhagen, Denmark). After incubation in triplicate with 200 μ l culture medium for 72 h at 37 °C, humidified air that contained 5% CO₂, 10 μ l of Concanavalin A (Con A, Sigma) was added to the wells to give a final concentration of 5 μ g/ml Con A. After incubation, triplicate wells for each experiment were pulsed for a final 18 h with 1 μ Ci of ³H-thymidine (specific activity 42 Ci/mmol; Amersham, Arlington Heights, IL, USA). An automatic cell harvester gathered the cells onto glass fiber filters. The amount of radioactivity incorporated into the DNA was determined in a liquid scintillation spectrometer (Wallac Micro Beta[®] TriLux, PerkinElmer, Waltham, MA, USA).

Assay of apoptotic fragmentation

To identify the effect of APG on the IR-triggered apoptosis of jejunum crypt cells, small intestines were separated from mice (n = 10/group) at 24 h after 2 Gy or 7 Gy WBI and fixed in 10% buffered formalin. The blocks were then embedded in paraplast wax to prepare 5 µm sections for hematoxylin and eosin (H&E) staining. Apoptosis was assessed on the evidence of morphological characteristics, such as cell shrinkage, chromatin condensation and margination and cellular fragmentation as described by jee et al. (2005). To confirm apoptotic crypt cells, TdT-mediated dUTP-biotin nick end labeling (TUNEL) assay was performed using a commercial apoptosis detection kit (ApopTag[®] Peroxidase *In Situ* Apoptosis Detection Kit, Chemicon International, Temecula, CA, USA) according to the manufacturer's instructions. Apoptotic crypt cells from small intestine sections of each mouse were counted using a light microscope and 50 crypts per intestinal section were recorded.

Tissue processing and immunohistochemistry

The jejunum was removed from mice killed 24 h after 7 Gy WBI and fixed in 10% neutral buffered formalin for 24 h. They were then processed for embedding vertically in paraplast wax; four different parts of the jejunum were prepared. Sections (5 µm-thick) were dewaxed in xylene (5 min with constant agitation) and rehydrated through a series of ethanol (95, 90, 80, and 70%). They were then immersed in 0.3% hydrogen peroxide in distilled water for 20 min to block endogenous peroxidase activity. After three washes in PBS (5 min), sections were pre-blocked in 10% normal goat serum (VECTASTAIN Elite ABC kit; Vector, Burlingame, CA, USA) then reacted with antibody to p53 (1:200 dilution, Calbiochem, Darmstadt, Germany), Bax (1:500 dilution, Cell Signaling Technology Inc, Beverly, MA, USA), Bcl-2 (1:500 dilution, Santa Cruz Biotechnology, Santa Cruz, CA, USA), Bcl-X_{SL} (1:500 dilution, Santa Cruz Biotechnology), Cytochrome C (1:400 dilution, Cell Signaling Technology Inc) or Cleaved Caspase-3 (1:25 dilution, Cell Signaling Technology Inc) for 1 h. After three washes, the sections were then

incubated with biotinylated anti-mouse or mouse IgG antibody (Vector) for 45 min, and then avidin-biotin peroxidase complexes were formed using an Elite kit (Vector). HRP-binding sites were detected with 3, 3'-diaminbenzidine (DAB; Vector) and counterstained with hematoxylin.

Image analysis and statistics

The positive cells on a specimen was semi-quantitatively estimated: negative (0) – none of the positive cells at 400× magnification; weak positive (1) – visible cells only at 400× magnification; moderate positive (2) – easy distinguished cells at low magnification 100×; intense positive (3) – cells intense positive at 100×magnification. Quantifying positive cells stained by immunohistochemistry was done using Image J 1.38× software. All data were presented as means ± standard error of the mean (S.E.M.), P values were determined using the one-way analysis of variance or Kruskal-Wallis test followed by Scheffe test. P value less than or equal to 0.05 was considered to indicate statistical significance.

4. RESULTS

APG improved hemopoiesis in γ -ray irradiated mice

CFU assay was performed to assess whether APG can rescue hemopoietic cells in gamma ray irradiated mice. As Fig. 1 depict, there are no colonies in spleens of mice of non-irradiated group. However, in spleens given with sub-lethal dosed of γ -ray irradiation (7 Gy) (the only 7 Gy-irradiated group), few endogenous colonies were found (5.8) and their sizes were markedly reduced, compared to non-irradiated mice. In contrast, the treatment of APG increased the size of spleen and the number of endogenous CFUs, when compared with the non-treated irradiated mice (8.3 in APG-plus 7 Gy-irradiated mice). After 30 days of the exposure to gamma ray irradiation, spleens enlarged by APG treatment reverted back to normal size (data not shown). These results indicate that APG led to the hemopoietic effects in gamma ray irradiated mice.

APG reduced DNA damage in peripheral blood lymphocytes

We studied the influence of APG on DNA damage to peripheral blood lymphocytes caused by IR using alkaline comet assay. We measured the DNA damage in the tails of APG plus irradiated (Fig. 2C) and non-irradiated (Fig. 2A) mice, as compared to the only γ -ray irradiated group (Fig. 2B). Fig. 2D showed the changes in the levels of DNA damage in non- irradiated group, γ -ray irradiated group, and APG plus irradiated group, respectively. Significant decrease in the levels of DNA damage was observed in APG treated group when compared with non-irradiated group. There was a significant decrease in the levels of DNA (%) in tail: 42.1 ± 8.7 vs. 19.9 ± 5.7 ($p < 0.05$). These results show that APG might reduce the DNA damages of the peripheral blood lymphocytes caused by IR.

APG inhibited apoptosis of peripheral blood lymphocytes

Since peripheral blood lymphocytes are one of the most sensitive cells to IR (Hrycek and Stieber. 1994), we assessed the nuclear morphology of peripheral blood lymphocytes from irradiated mice with and without APG treatment to determine whether the inhibition of their DNA damage was attributable to apoptotic changes. As shown Fig. 3A, DAPI staining revealed that nuclei of peripheral blood lymphocytes undergoing apoptosis had significant fragmentation and condensation of nuclei after an exposure to IR. The recipients of APG manifested a dramatically decreased the number of apoptotic nuclei compared to that of the Non irradiated group (Fig. 3B and 3C) (11.7 ± 0.7 vs. 17.0 ± 1.4 , $p < 0.05$). These results suggest that APG inhibited the damages of peripheral blood lymphocytes by reducing the formation of apoptosis caused by γ -ray irradiation.

APG induces proliferation and stimulates differentiation of splenocytes

Next, to determine whether APG stimulates splenocyte's proliferation against γ -ray irradiation, the ^3H -thymidine incorporation assay was performed. The proliferation of splenocytes was markedly reduced by an exposure to γ -ray irradiation when compared with non-irradiated cells (Fig. 4). Interestingly, the treatment of APG resulted in about 3 days 5.1-fold, 9 days 10.2-fold, and 13 days 10.4-fold increases of splenocytes respectively in comparison with 2 Gy-irradiated and non-treated cells ($p < 0.05$). These results suggest that APG stimulated the splenocyte's proliferation against γ -ray irradiation.

APG inhibits irradiation-induced apoptosis

We then tested small intestinal crypt cells for inhibition of radiation-induced apoptosis after APG treatment. The apoptotic cells were observed in the putative

stem cell zone located towards the bottom of the small intestinal crypts and easily recognized from the condensation of cytoplasm and nuclear fragments through both H&E staining (Fig. 5A, B) and the TUNEL assay (Fig. 5C, D). After WBI, the number of apoptotic cells rose sharply with an increasing dose of γ -ray. As shown in Fig. 5E, radiation alone at 2 and 7 Gy linearly increased apoptosis to peaks of 3.8 ± 0.1 and 11.6 ± 2.5 per crypt, respectively (vs. $0.4 \pm 0.01\%$ in non-irradiated control). However, APG treatment with irradiation resulted in a significant decrease in the number of apoptotic crypt cells, compared with those in the irradiation control group (2.51 ± 0.1 vs. 6.3 ± 1.1 , $p < 0.05$) (Fig. 5B, D). The results using TUNEL assay had a similar trend to that seen after H&E staining ($2.41 \pm 0.03\%$ vs. $1.87 \pm 0.21\%$ from APG treated control vs. untreated control groups, $p < 0.05$). The frequency of spontaneous apoptosis in crypt cells of non-irradiated animals was not significantly different from that of APG-only-treated animals (data not shown). This indicates that APG offers protection against radiation-induced apoptosis in the intestinal crypts.

APG attenuated the immunohistochemical localization and intensity of p53 in the intestine

To understand the mechanism by which APG inhibits the apoptosis in the small intestine following radiation exposure, we first investigated the localization and intensity of p53 pro-apoptotic proteins, which are activated by single- and double-strand breaks from irradiation. In most cases, p53 exhibited a marked granular punctuate pattern found both in the nuclei and cytoplasm of the intestinal cells. As shown in Fig. 6, the immunoreactivity of p53 was markedly increased in the irradiated control compared to the non-irradiated control, but was significantly reduced in APG plus irradiated group compared to the irradiated control by 83.0% (Fig. 6H). Immunoreactive p53 positive cells were abruptly increased in the lamina propria and crypt (Fig. 6C, D and G) compared to the sham-irradiated controls (Fig. 6A, B and G). Conversely, immunoreactive positive cells were sharply decreased in APG plus

irradiated group (Fig. 6E, F and G).

APG modulated the immunohistochemical localization and intensity of Bcl-2 family proteins in the intestine

Next, we investigated the localization and intensity of Bcl-2 family proteins which govern mitochondrial outer membrane permeabilization following radiation exposure. As shown in 7-9 an exposure to irradiation considerably increased the expression of pro-apoptotic Bcl-2 family protein, Bax (Fig. 7) but decreased the expression of anti-apoptotic Bcl-2 family proteins such as Bcl-2 (Fig. 8) and Bcl-X_{S/L} (Fig.9) compared to the non-irradiated controls. However, APG treatment distinctly curtailed the increase of Bax expression levels and the decrease of Bcl-2 and Bcl-X_{S/L} expression in APG plus irradiated group exhibited a 34.0% and 33.3% increment compared to the irradiated controls, respectively (Figs. 8H and 9H).

When irradiated, immunoreactive Bax positive cells were confined to the cytoplasm of apoptotic cells with diverse morphology and found predominantly in intestinal epithelia and crypt cells. Accordingly, Bax immunoreactivity was summarily increased in apoptotic cells, mostly in the epithelial region of the irradiated control group (Fig. 7C, D and G) and gradually decreased in the APG plus irradiated group (Fig. 7E, F and G).

As with immunoreactive staining patterns of Bax proteins, characteristic Bcl-2 and Bcl-X_{S/L} staining was observed in the cytoplasm of intestinal cells under irradiation. Intriguingly, Bcl-2 displayed a distinctly different localization in nuclei in the lamina propria of irradiated controls (Fig. 8C, D and G) and in the APG plus irradiated group (Fig. 8E, F and G) compared with the non-irradiated group, where it was restricted to the cytoplasm in epithelia and the lamina propria (Fig. 8A, B and G). Bcl-X_{S/L} immunostaining was moderate in all the normal tissues and was observed mostly in the cytoplasm. But the pattern looked more granular in appearance and

was clearly different from the pattern of Bcl-2 expression pattern (Fig. 9). In contrast to the reduced Bax immunoreactivity, the number of Bcl-2 positive cells and the intensity of Bcl-2 in APG plus irradiated group barely rose compared with those of the irradiated controls. Accompanying these changes, more intense Bcl-X_{S/L} immunoreactivity was easily demarcated in the cytoplasm of intestinal epithelium in APG plus irradiated group (Fig. 9E, F and G) than in the irradiated control group (Fig. 9C, D and G). These results suggest that APG presumably inhibited the apoptosis of the small intestine by regulating the expression of Bcl-2 family proteins after gamma ray irradiation.

APG abated the immunohistochemical localization and intensity of Cytochrome C in intestine

Then we investigated the localization and intensity of Cytochrome C which was released by the mitochondria in response to pro-apoptotic stimuli. As shown in Fig. 10, the expression levels of Cytochrome C increased more than fourteen-fold in the irradiated control compared to non-irradiated controls, but were reduced by 64.8% in the APG plus irradiated group compared with the irradiated controls (Fig. 10H). The immunostaining of Cytochrome C was easily identified in the irradiated control group from its clear trace in the cytoplasmic component of the intestinal cell and crypt (Fig. 10C, D and G). This overexpression of Cytochrome c after irradiation was significantly decreased by APG treatment (Fig. 10E, F and G). These results indicate that the attenuated expression of Cytochrome C after APG treatment was presumably inhibited the mitochondria mediated apoptosis in the small intestine following irradiation.

APG diminished the immunohistochemical localization and intensity of Caspase-3 cleavage in intestine

Finally, we investigated the localization and intensity of cleaved Caspase-3, which is activated in the apoptotic cell by mitochondrial pathways. As shown in Fig. 11, the expression level of cleaved Caspase-3 was markedly increased in the small intestine of the irradiated control compared to the non-irradiated control. However, APG plus irradiated group presented a 31.3% decrease of cleaved Caspase-3 expression compared to that of irradiated controls (Fig. 11H). A greater distribution of cleaved Caspase-3 positive cells was exhibited in the apoptotic crypt cells of the small intestine mostly in the irradiation control group (Fig. 11C, D and G) whereas the non-irradiated cells exhibited faint and infrequent immunoreactive staining (Fig. 11A, B and G). Irradiation enhanced the cleaved Caspase-3 positive cells, but APG treatment markedly reduced the number of cleaved Caspase-3 positive cells and apoptotic cells in the crypt (Fig. 11E, F and G).

APG improves the survival rate of mice exposed to a lethal dose of irradiation

To test whether APG could protect mice from radiation induced damages, APG was administered at doses of 10 mg/kg b.w. at 2 and 18 h before exposure to 9 Gy of WBI. Only 44.4% (9/21) of the irradiated, untreated group survived for 30 days after exposure to 9 Gy of irradiation. However, 84.6% (11/13) of the mice that received APG plus irradiation survived for 30 days, which represents a significantly diminished death rate (Table 2). These results demonstrate that APG confers marked radioprotection and subsequently prolongs the survival of lethally irradiated mice.

5. DISCUSSION

In general, proliferating stem or progenitor cells are particularly vulnerable to radiation-induced cell damage, a prominent example being the stem cells in the hemopoietic systems (Potten and Grant. 1998). And the gastrointestinal (GI) system is a major target for the somatic injuries incurred by radiation and chemotherapy, it is important to protect the intestine from radiation-induced damage, the main cause of radiation-induced intestinal damage, for diminishing side effects induced by irradiation (Hosseinimehr. 2007). Several studies have reported that the exposure of animals to radiation leads to the destruction of the lymphoid and hemopoietic systems by increasing apoptosis of not only peripheral blood lymphocytes but also splenocytes known to be radio sensitive cells in peripheral immune systems (Andreson and Warner. 1976; Hagelstrom et al. 1995). Also, our previous studies demonstrated that radio-protective agents from natural resources can protect small intestines from radiation-induced apoptosis and they further elucidated their mechanisms of anti-apoptotic effects (Park et al. 2008b; Thotala et al. 2009; Bonnaud et al. 2010). In addition, APG has protective effects against radiation-induced intestinal damage by enhancing intestinal crypt regeneration and inhibiting irradiation-induced apoptosis.

In this study, we extended our previous research on APG's molecular mechanism of protective effect against radiation-induced apoptosis in small intestine and peripheral immune tissue damage by radiation exposure. So, we demonstrate that APG effectively protects mice against potentially lethal irradiation and prolongs the survival of lethally irradiated animals. The survival time for lethally irradiated animals can be lengthened by various manipulations, such as inhibition of free radical generation or acceleration of their removal, enhancement of DNA repair, replenishment of dead hematopoietic cells, and stimulation of immune cell formation or activity (Arora et al. 2005). However, no other reports to date have described the protective effect of APG against radiation-induced peripheral immune tissue and small

intestine damage or the apoptosis mechanism of that effect in vivo. Radiation-induced oxidative damage to DNA encompasses several types of base damage and single- or double-strand breaks (Nair et al. 2001). Using the comet assay, we observed that APG treatment significantly decreased the percentage of tail DNA fluorescence in the peripheral blood lymphocytes of irradiated mice, which indicates that APG protected cells against radiation-induced damage. This decrease in DNA breakage seen in our APG-treated, irradiated mice underlines the cytoprotective efficacy of this compound in vivo, which may be attributed to its ROS scavenging activity.

Hematopoietic stem cells are highly sensitive to IR as well as chemotherapeutic drugs administered to cancer patients. In fact, myelosuppression and hematopoietic dysfunction are the most common clinical complications of these treatments (Chen et al. 2007). Therefore, an important adjunct to their use is to promote the recovery of hematopoiesis (Neta et al. 1986). In our experiments, mice treated with eckol recovered from WBI as established by their increased numbers of splenic CFUs in comparison with the irradiated controls that did not receive APG. The enhancement of endogenous CFUs in mice that received APG before undergoing irradiation indicates that APG protects and/or stimulates the proliferation of hematopoietic stem cells. This important mechanism of APG-mediated survival described here appears to have a strong potential for clinical application.

It is well recognized that a major mechanism of radiation induced apoptosis involves p53, a tumor suppressor protein related to cell cycle arrest and apoptosis (Gudkov and Komarova. 2010). Although the role of p53 in the small intestine of irradiated mice remains unclear, it is considered that the pro-apoptotic function of p53 could determine general radiosensitivity (Gudkov and Komarova. 2010). Furthermore, previous reports demonstrated that p53 in cytoplasm directly regulates the Bax-dependent mitochondrial pathway to apoptosis (Geng et al. 2010). In the current study, we observed that the expression levels and localization of p53 were significantly down-regulated in the APG plus irradiated group compared to irradiated control, which showed distinctively elevated expression and localization of p53.

Consistent with our previous study, the distribution pattern of p53 was found in both the nuclei and cytoplasm of the small intestinal cells (Ha et al. 2013), which could explain that p53 inhibition by APG treatment in WBI mice might affect the Bax-dependent mitochondrial pathway.

In response to apoptotic signals from p53 activation, Bax, one of representative pro-apoptotic Bcl-2 family proteins, promotes mitochondrial outer membrane permeabilization (MOMP) via forming the oligomerization in the outer mitochondrial membrane (Vousden and Lane. 2007). Mitochondria play a crucial role in amplifying apoptotic signals, through which MOMP induces the release of Cytochrome C from the intermembrane space. However, this MOMP can be blocked by anti-apoptotic proteins of the Bcl-2 family, Bcl-2 and Bcl-X_{SL}, which play an important role in antagonizing apoptosis by preventing the pro-apoptotic signal transmission of pro-apoptotic genes (Van Delft and Huang. 2006). The Bcl-2 family of pro-apoptotic and anti-apoptotic proteins serve as pivotal death regulators that reside upstream of mitochondria, modulating the expression of Bcl-2 family is significant in mitigating radiation induced damage. In present study, the expression level of pro-apoptotic molecule Bax was down-regulated in the APG plus irradiated group, while the anti-apoptotic molecules Bcl-2 and Bcl-X_{SL} were greater in APG-treated mice than irradiated controls. The immunohistochemical expression pattern and localization of these proteins were consistent with our previous study (Ha et al. 2013).

Cytochrome C released from mitochondria contributes to the formation of the apoptosome and further causes cleavage of pro-Caspase-3 to cleaved Caspase-3 (Cotter. 2009). However, the expression level and immunohistochemical localization of Cytochrome C was significantly decreased by treatment of APG compared to irradiated control, which implies that pro-apoptotic properties of Cytochrome C after irradiation were interrupted by the APG treatment.

Since cleaved Caspase-3 is the predominant downstream executioner caspase, it was designated as the target caspase (Budihardjo et al, 1999). Furthermore, immunohistochemical detection of cleaved Caspase-3 was suggested as a suitable

alternative method to quantify radiation-induced apoptosis (Marshman et al. 2001). In the current study, APG treatment markedly reduced the number of cleaved Caspase-3 positive cells and apoptotic cells in the crypt after irradiation. The expression of cleaved Caspase-3 was reported to exist preferentially in crypts in small intestine of irradiated mice (Przemeck et al. 2007; Vyas et al. 2007). These data indicate that APG treatment could enhance the protection of small intestine from radiation damage by inhibiting caspase-dependent apoptosis. Incidentally, it is reported that mitochondria, as the cross-talk organelle, connect the two major apoptosis pathway, caspase-dependent and caspase-independent pathways. While these results demonstrate that anti-apoptotic effect of APG was mediated through the inhibition of Caspase-3 activation, the possibility still remains that APG treatment regulates other caspase-independent apoptosis pathway molecules.

In conclusion, these results demonstrate that APG protects mice against oxidative stress from IR by enhancing hematopoiesis and promoting cell survival via inhibiting DNA damages through the regulation of apoptosis in peripheral blood lymphocytes and splenocytes. Futhermore, APG blocks the p53-dependent pathway and mitochondria/caspase-dependent pathway in irradiated small intestine, which ultimately results in beneficial effects against from radiation induced damage. This study indicates that APG may serve as a beneficial protective agent for human recipients of IR.

6. REFERENCES

- Anderson RE, Warner NL. 1976. Ionizing radiation and the immune response. *Adv Immunol* 24:215–335.
- Arora R, Gupta D, Chawla R, Sagar R, Sharma A, Kumar R, Prasad J, Singh S, Samanta N, Sharma RK. 2005. Radioprotection by plant products: present status and future prospects. *Phytother Res* 19(1):1–22.
- Bogo V, Jacobs AJ, Weiss JF. 1985. Behavioral toxicity and efficacy of WR-2721 as a radioprotectant. *Radiat Res* 104(2):182–190.
- Bonnaud S, Niaudet C, Legoux F, Corre I, Delpon G, Saulquin X, Fuks Z, Gaugler MH, Kolesnick R, Paris F. 2010. Sphingosine-1-phosphate activates the AKT pathway to protect small intestines from radiation-induced endothelial apoptosis. *Cancer Res* 70(23):9905–9915.
- Budihardjo I, Oliver H, Lutter M, Luo X, Wang X. 1999. Biochemical pathways of caspase activation during apoptosis. *Annu Rev Cell Dev Biol* 15:269–290.
- Chen T, Burke KA, Zhan Y, Wang X, Shibata D, Zhao Y. 2007. IL-2 facilitates both recovery of endogenous hematopoiesis and the engraftment of stem cells after ionizing radiation. *Exp Hematol* 35(2):203–213.
- Cotter TG. 2009. Apoptosis and cancer: the genesis of a research field. *Nat Rev Cancer* 9(7):501–507.
- Geng Y, Walls KC, Ghosh AP, Akhtar RS, Klocke BJ, Roth KA. 2010. Cytoplasmic p53 and activated bax regulate p53-dependent, transcription-independent neural precursor cell apoptosis. *J Histochem Cytochem* 58(3):265–275.
- Gudkov AV, Komarova EA. 2010. Pathologies associated with the p53 response. *Cold Spring Harb Perspect Biol* 2(7):a001180.

- Ha D, Bing SJ, Cho J, Ahn G, Kim DS, Al-Amin M, Park SJ, Jee Y. 2013. Phloroglucinol protects small intestines of mice from ionizing radiation by regulating apoptosis-related molecules: a comparative immunohistochemical study. *J Histochem Cytochem* 61(1):63–74.
- Hagelström AH, Gorla NB, Larripa IB. 1995. Chromosomal damage in workers occupationally exposed to chronic low level ionizing radiation. *Toxicol Lett* 76(2):113–117
- Hosseinimehr SJ. 2007. Trends in the development of radioprotective agents. *Drug Discov Today*. 12(19-20):794–805
- Hrycek A, Stieber M. 1994. Selected issues related to the effect of ionizing radiation on leukocytes, particularly neutrophilic granulocytes. *Wiad Lek* 47(7-8):288–291.
- Hwang I, Ahn G, Park E, Ha D, Song JY, Jee Y. 2011. An acidic polysaccharide of *Panax ginseng* ameliorates experimental autoimmune encephalomyelitis and induces regulatory T cells. *Immunol Lett* 138(2):169–178.
- Jee YH, Jeong WI, Kim TH, Hwang IS, Ahn MJ, Joo HG, Hong SH, Jeong KS. 2005. p53 and cell-cycle-regulated protein expression in small intestinal cells after fast-neutron irradiation in mice. *Mol Cell Biochem* 270(1-2):21–28.
- Kim MM, Kim SK. 2010. Effect of phloroglucinol on oxidative stress and inflammation. *Food Chem Toxicol* 48(10):2925–2933.
- Kim HJ, Kim MH, Byon YY, Park JW, Jee Y, Joo HG. 2007. Radioprotective effects of an acidic polysaccharide of *Panax ginseng* on bone marrow cells. *J Vet Sci* 8(1):39–44.
- Lee TK, O'Brien KF, Wang W, Sheng C, Wang T, Johnke RM, Allison RR. 2009. American ginseng modifies 137Cs-Induced DNA damage and oxidative stress in human lymphocytes. *Open Nucl Med J* 1(1):1–8.

- Marshman E, Ottewell PD, Potten CS, Watson AJM. 2001. Caspase activation during spontaneous and radiation-induced apoptosis in the murine intestine. *J Pathol* 195(3):285–292.
- Mashiba H, Yoshinaga H, Matsunaga K, Gojobori M, Furusawa M. 1979. Effect of immunochemotherapy on lymphocyte response of patients with gastrointestinal cancer. *J Surg Oncol* 12(3):275–279.
- Moon C, Kim SH, Kim JC, Hyun JW, Lee NH, Park JW, Shin T. 2008. Protective effect of phlorotannin components phloroglucinol and eckol on radiation-induced intestinal injury in mice. *Phytother Res* 22(2):238–242.
- Moulder JE. 2003. Pharmacological intervention to prevent or ameliorate chronic radiation injuries. *Semin Radiat Oncol* 13(1):73–84.
- Moulder JE. 2002. Report on an interagency workshop on the radiobiology of nuclear terrorism. Molecular and cellular biology of moderate dose (1–10 Sv) radiation and potential mechanisms of radiation protection. *Radiat Res* 158(1):118–124.
- Nair CK, Parida DK, Nomura T. 2001. Radioprotectors in radiotherapy. *J Radiat Res* 42(1):21–37.
- Neta R, Douches S, Oppenheim JJ. 1986. Interleukin 1 is a radioprotector. *J Immunol* 136(7):2483–2485.
- Park E, Ahn GN, Lee NH, Kim JM, Yun JS, Hyun JW, Jeon YJ, Wie MB, Lee YJ, Park JW, Jee Y. 2008a. Radioprotective properties of eckol against ionizing radiation in mice. *FEBS Lett* 582(6):925–930.
- Park E, Lee NH, Joo HG, Jee Y. 2008b. Modulation of apoptosis of eckol against ionizing radiation in mice. *Biochem Biophys Res Commun* 372(4):792–797.
- Park E, Ahn G, Yun JS, Kim MJ, Bing SJ, Kim DS, Lee J, Lee NH, Park JW, Jee Y. 2010. Dieckol rescues mice from lethal irradiation by accelerating hemopoiesis

- and curtailing immunosuppression. *Int J Radiat Biol* 86(10):848–859.
- Pellmar TC, Rockwell S; Radiological/Nuclear Threat Countermeasures Working Group. 2005. Priority list of research areas for radiological nuclear threat countermeasures. *Radiat Res* 163(1):115–123.
- Potten CS, Grant HK. 1998. The relationship between ionizing radiation-induced apoptosis and stem cells in the small and large intestine. *Br J Cancer* 78(8):993–1003.
- Przemeck SMC, Duckworth CA, Pritchard DM. 2007. Radiation-induced gastric epithelial apoptosis occurs in the proliferative zone and is regulated by p53, bak, bax, and bcl-2. *Am J Physiol Gastrointest Liver Physiol* 292(2):G620–627.
- Satoh S, Suzuki A, Okamura H, Nishimura T. 1982. Case of malignant melanoma of the external genitalia responding satisfactorily to a combination of local injection of OK-432 and chemotherapy. *Gan To Kagaku Ryoho* 9(1):140–145.
- Stone HB, Moulder JE, Coleman CN, Ang KK, Anscher MS, Barcellos-Hoff MH, Dynan WS, Fike JR, Grdina DJ, Greenberger JS, Hauer-Jensen M, Hill RP, Kolesnick RN, Macvittie TJ, Marks C, McBride WH, Metting N, Pellmar T, Purucker M, Robbins ME, Schiestl RH, Seed TM, Tomaszewski JE, Travis EL, Wallner PE, Wolpert M, Zaharevitz D. 2004. Models for evaluating agents intended for the prophylaxis, mitigation and treatment of radiation injuries. Report of an NCI Workshop, December 3-4, 2003. *Radiat Res* 162(6):711-728.
- Song JY, Han SK, Bae KG, Lim DS, Son SJ, Jung IS, Yi SY, Yun YS. 2003. Radioprotective effects of ginsan, an immunomodulator. *Radiat Res* 159(6):768–774.
- Song JY, Han SK, Son EH, Pyo SN, Yun YS, Yi SY. 2002. Induction of secretory and tumoricidal activities in peritoneal macrophages by ginsan. *Int Immunopharmacol* 2(7):857–865.

- Shin JY, Song JY, Yun YS, Yang HO, Rhee DK, Pyo S. 2002. Immunostimulating effects of acidic polysaccharides extract of *Panax ginseng* on macrophage function. *Immunopharmacol Immunotoxicol* 24(3):469–482.
- Thotala D, Chetyrkin S, Hudson B, Hallahan D, Voziyan P, Yazlovitskaya E. 2009. Pyridoxamine protects intestinal epithelium from ionizing radiation-induced apoptosis. *Free Radic Biol Med* 47(6):779–785.
- Van Delft MF, Huang DCS. 2006. How the Bcl-2 family of proteins interact to regulate apoptosis. *Cell Res* 16(2):203–213.
- Vousden KH, Lane DP. 2007. p53 in health and disease. *Nat Rev Mol Cell Biol* 8(4):275–83.
- Vyas D, Robertson CM, Stromberg PE, Martin JR, Dunne WM, Houchen CW, Barrett TA, Ayala A, Perl M, Buchman TG, Coopersmith CM. 2007. Epithelial apoptosis in mechanistically distinct methods of injury in the murine small intestine. *Histol Histopathol* 22(6):623–630.
- Weiss JF. 1997. Pharmacologic approaches to protection against radiation-induced lethality and other damage. *Environ Health Perspect* 105(6):1473–1478.

Table 1. Immunohistochemical localization of different antibodies in the small intestine of mice subjected to Non IR, IR-control and IR+APG.

Antibody	Group	Localization		
		Crypt apoptotic cell	Intestinal epithelium	Lamina propria
P53	Non IR	-	-	+
	IR	++	-	+++
	IR+APG	-	-	++
Bax	Non IR	-	+	-
	IR	++	+++	-
	IR+APG	+	++	-
Bcl-2	Non IR	-	-	++
	IR	+	-	-
	IR+APG	+	-	+++
Bcl-X _{S/L}	Non IR	-	++	-
	IR	+	+	-
	IR+APG	+	+++	-
Cytochrome C	Non IR	-	-	-
	IR	+++	+	-
	IR+APG	++	-	-
Caspase3	Non IR	-	-	-
	IR	+++	-	-
	IR+APG	++	-	-

Stained sections were scored for the density of positive cells per field. -, negative; +, weak; ++, moderate; +++, intense.

Table 2. The effect of APG on survival rates after 9 Gy γ -ray irradiated mice.

Groups	survial rate(%)	Mean survial time(days)
9Gy Irradiation (n=21)	44.4	22.4 \pm 8.1
APG treated + 9 Gy irradiation (n=13)	84.6	24 \pm 10.2

Mice were injected with i.p. with APG (10 mg/kg b.w.) 2 and 18h before being exposed to 9 Gy of WBI. The term '*n*' represents the total number of mice in each group. The results shown are the means \pm S.D. of three independent experiments. Differences in the 30-day survival rates were calculated with Student's *t*-test ($p < 0.05$).

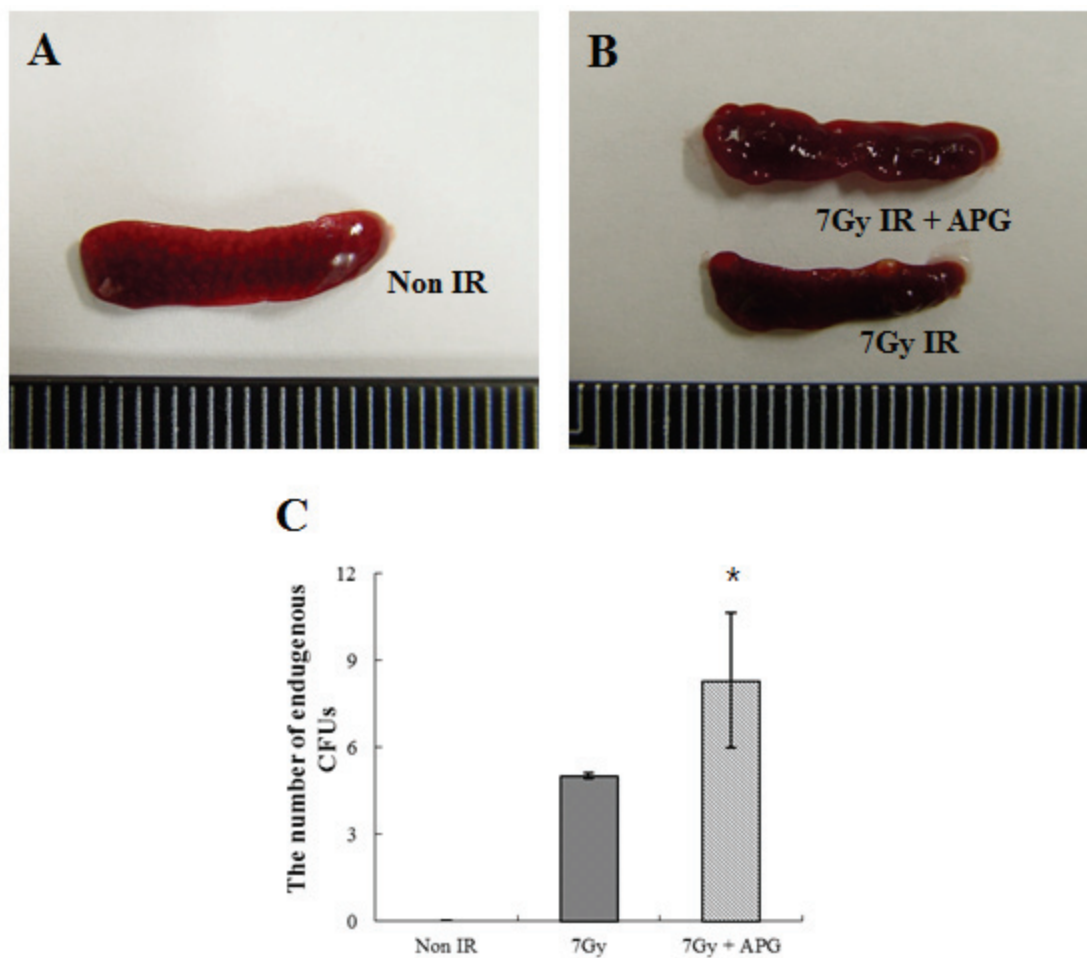


Figure 1. The effect of APG on survival rates after 9 Gy γ -ray irradiated mice. Photograph of spleens excised from naive mice (A), from control mice (no extract) given 7 Gy WBI and from test mice given 7 Gy irradiation plus APG (10mg/kg b.w., i.p.) (B). Each data point represents mean \pm SEM ($p < 0.05$). Although all spleens decreased in size after irradiation, the spleens of APG recipients were bigger and had more endogenous splenocyte colonies.

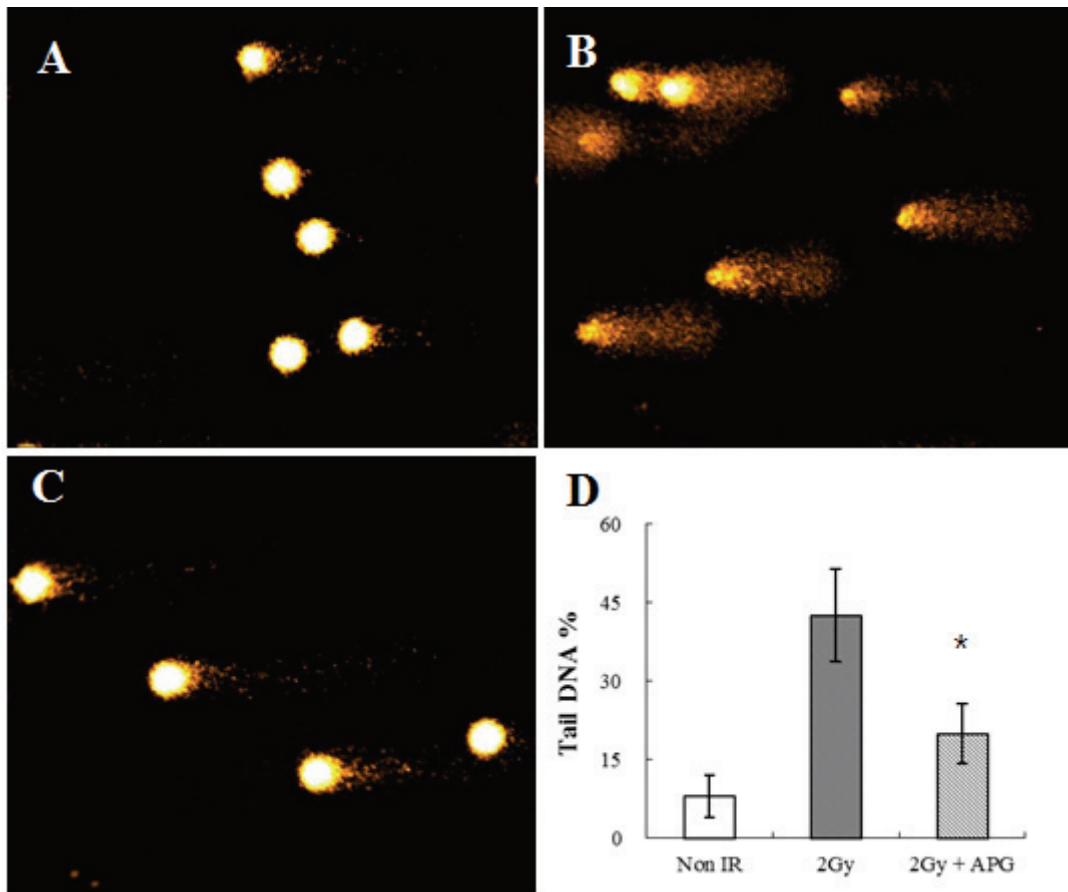


Figure 2. Comet assay of APG effect on irradiation-induced DNA damage in splenocytes comparing. Zero Gy irradiation (A), 2 Gy irradiation (B) and 2 Gy irradiation plus APG (10mg/kg b.w., i.p.) (C). The columns indicate percentages of tail DNA and of inhibition activity in each group (D). The cells are scored according to the Komet 5.5 program. Each data point represents mean \pm SD of about 50 cells per mouse. Inhibition activity was evaluated to compare the 2 Gy irradiation control group to the extract-treated irradiation group by using Student's *t*-test ($p < 0.05$).

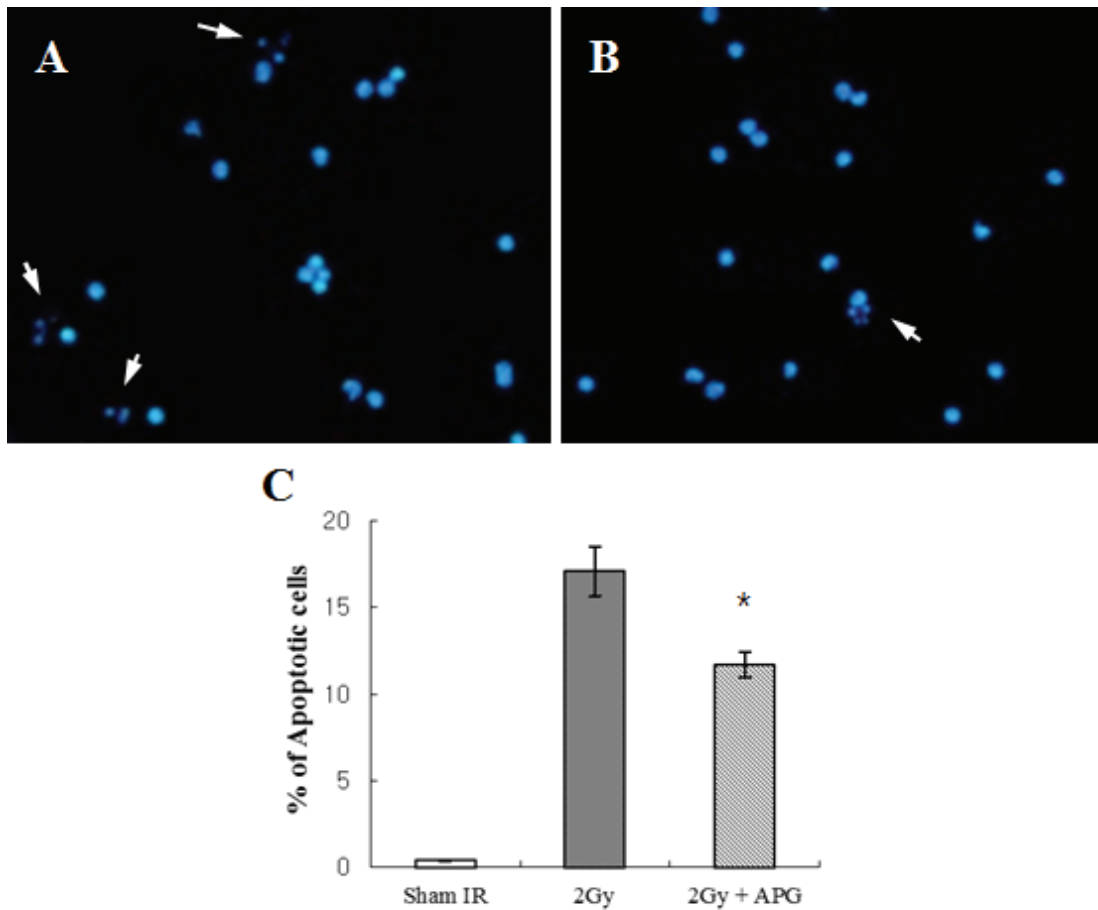


Figure 3. The effect of APG on apoptosis of splenocytes using DAPI staining. Mice were treated with 2 Gy irradiation alone (A) or 2 Gy irradiation plus APG (10mg/kg b.w., i.p.) (B). Columns indicate the number of apoptotic fragments in each group (C). Spleen were separated at 24hours after 2 Gy γ -ray irradiation. The arrows point to apoptotic cells with condensed and fragmented nuclei. Each data point represents the mean \pm SEM ($p < 0.05$).

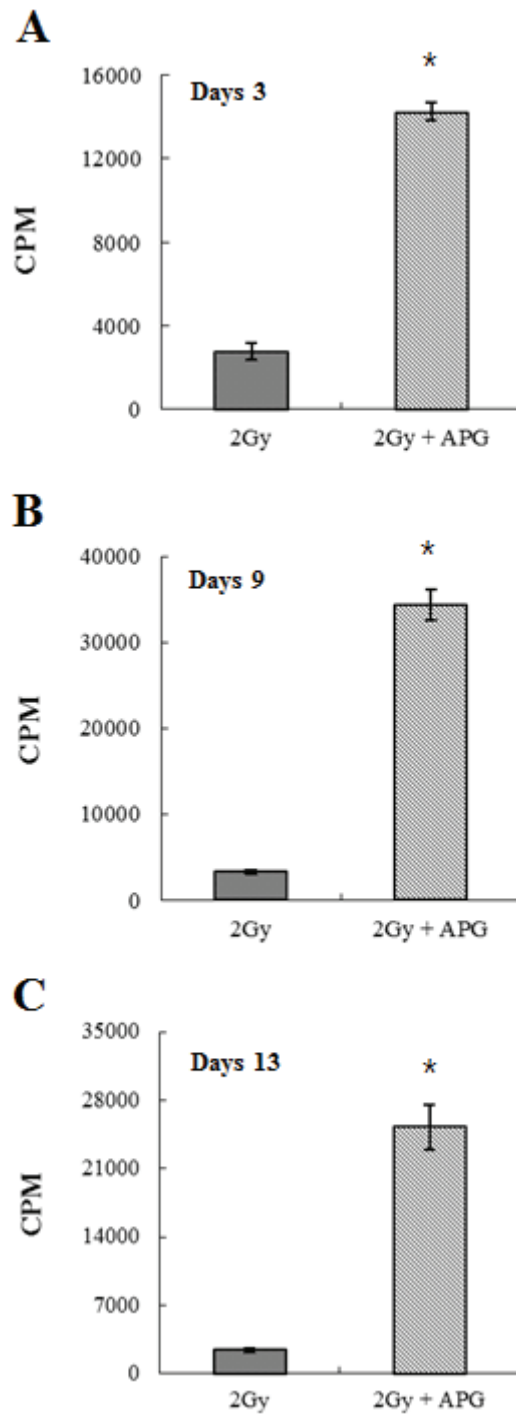


Figure 4. The effect of APG extract on proliferation of splenocytes. Splenocytes were isolated at 3 days (A), 9 days (B) and 13 days (C) after 2 Gy irradiation of mice.

APG extract was injected i.p. at 18 hours and 3 hours before irradiation. Irradiated cells (4×10^5 /well) were incubated with 200 μ l culture medium in 96-well culture plates for 72 hours in triplicate. The cells were pulsed for 18 hours with 1 μ Ci of 3 H-thymidine then harvested onto glass fiber filters, after which thymidine incorporation was measured. Each data point represents the mean \pm SEM. Statistical evaluation was performed to compare the extract-treated groups and corresponding untreated irradiated controls ($p < 0.05$).

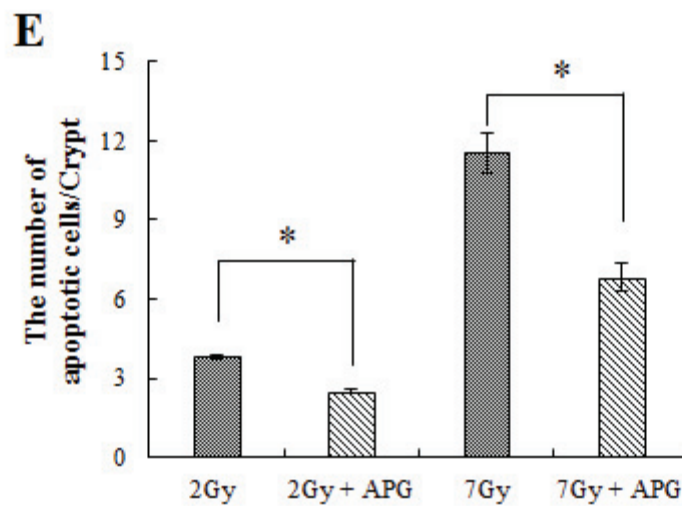
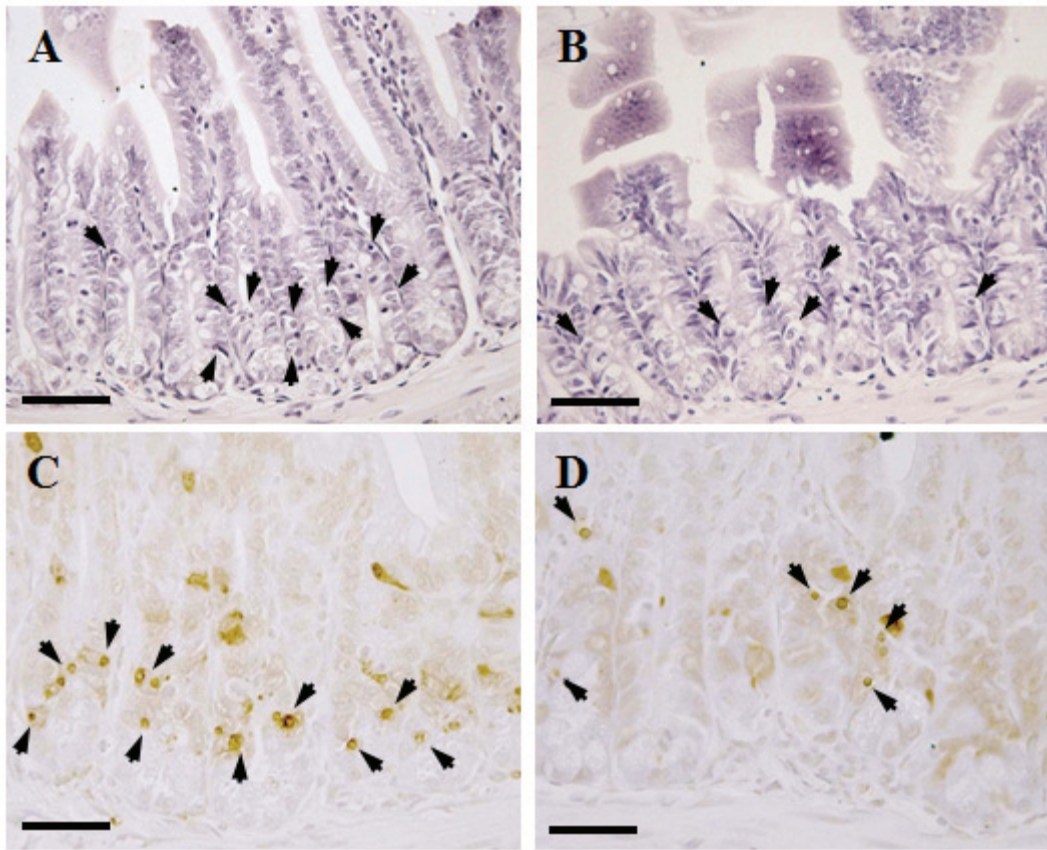
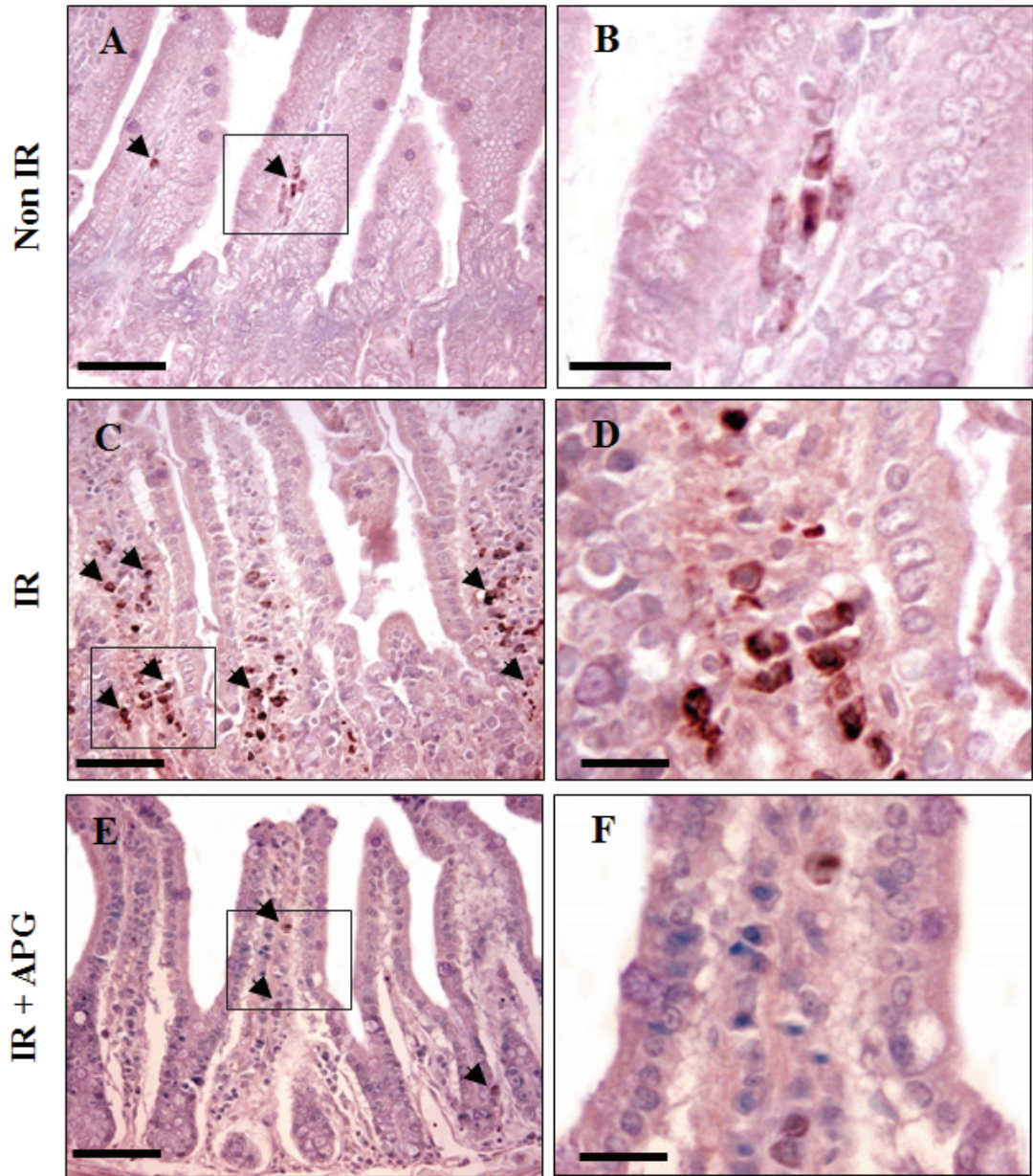


Figure 5. Representative images showing the apoptotic cells in the intestinal sections with H&E (A, B) and TUNNEL assay (C, D). The cells show chromatin condensation into crescentic caps at the nuclear periphery, nuclear disintegration and

shrinkage of cell volume by H&E (arrowheads). (A, C) 2 Gy irradiation, (B, D) 2 Gy irradiation plus APG (10 mg/kg b.w., i.p.) treated, (E) Columns represent the number of apoptotic fragments per small intestinal crypt in each group. The mice were sacrificed, and small intestines were obtained 24 h after 2 or 7 Gy γ -ray irradiation. Values are means \pm SE of 50 crypt sections per intestine and 5 small intestine sections from each mouse (Bars = 30 μ m, * p <0.05).



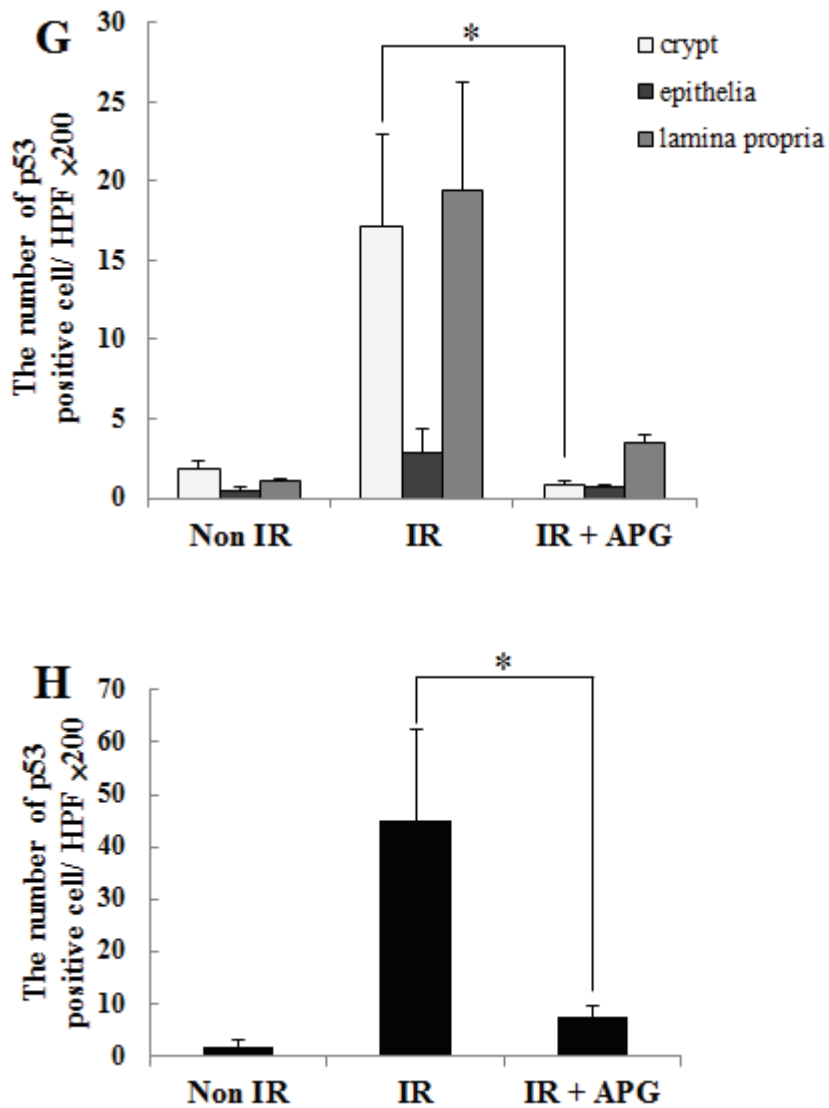
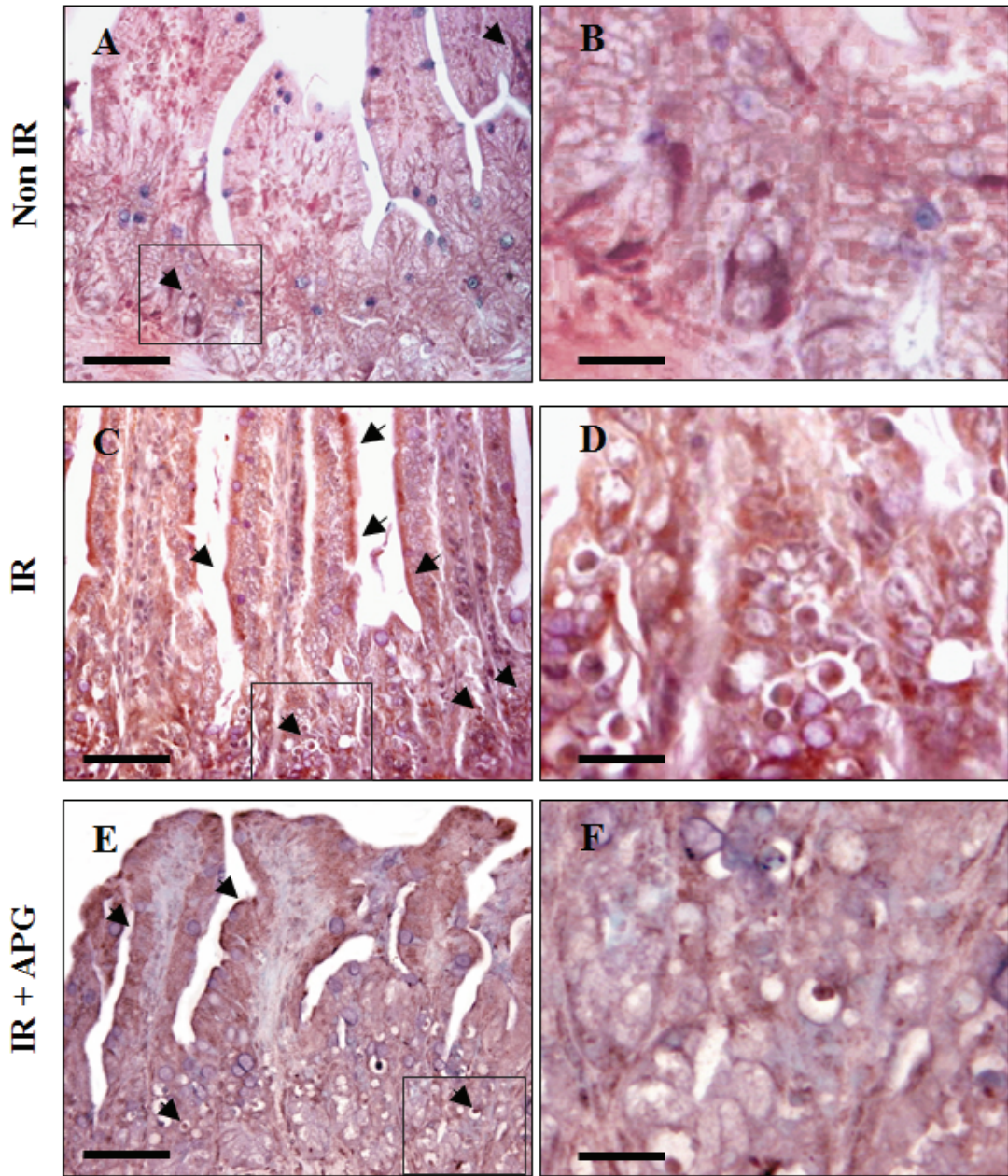


Figure 6. P53 immunoreactivity in small intestines of mice 24h after γ -ray irradiation. (A, B) Non irradiated-control, (C, D) Irradiated control, (E, F) APG plus irradiated group, (G) semi-quantitative analysis of immunohistochemistry for p53, (H) Quantitative analysis of immunohistochemistry for p53, (A, C, E) Bars = 60 μ m, (B, D, F) Bars = 30 μ m. (*; $P < 0.05$). Cells were counted as described in Materials and Methods. Results represent average and S.E. value in each experimental group. Data are representative of three independent experiments.



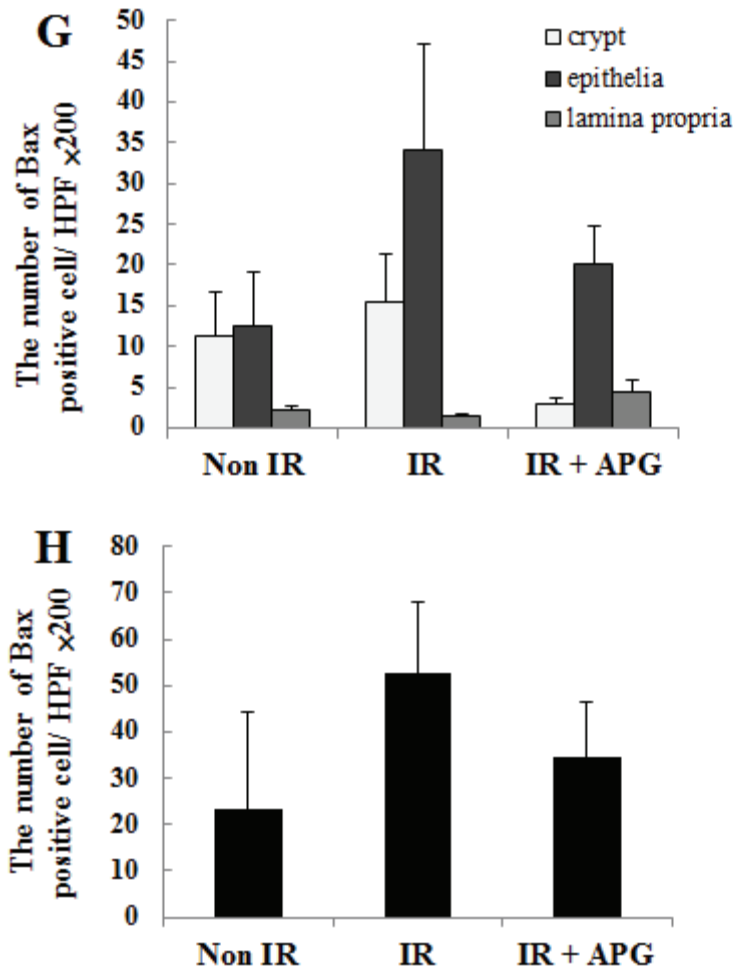
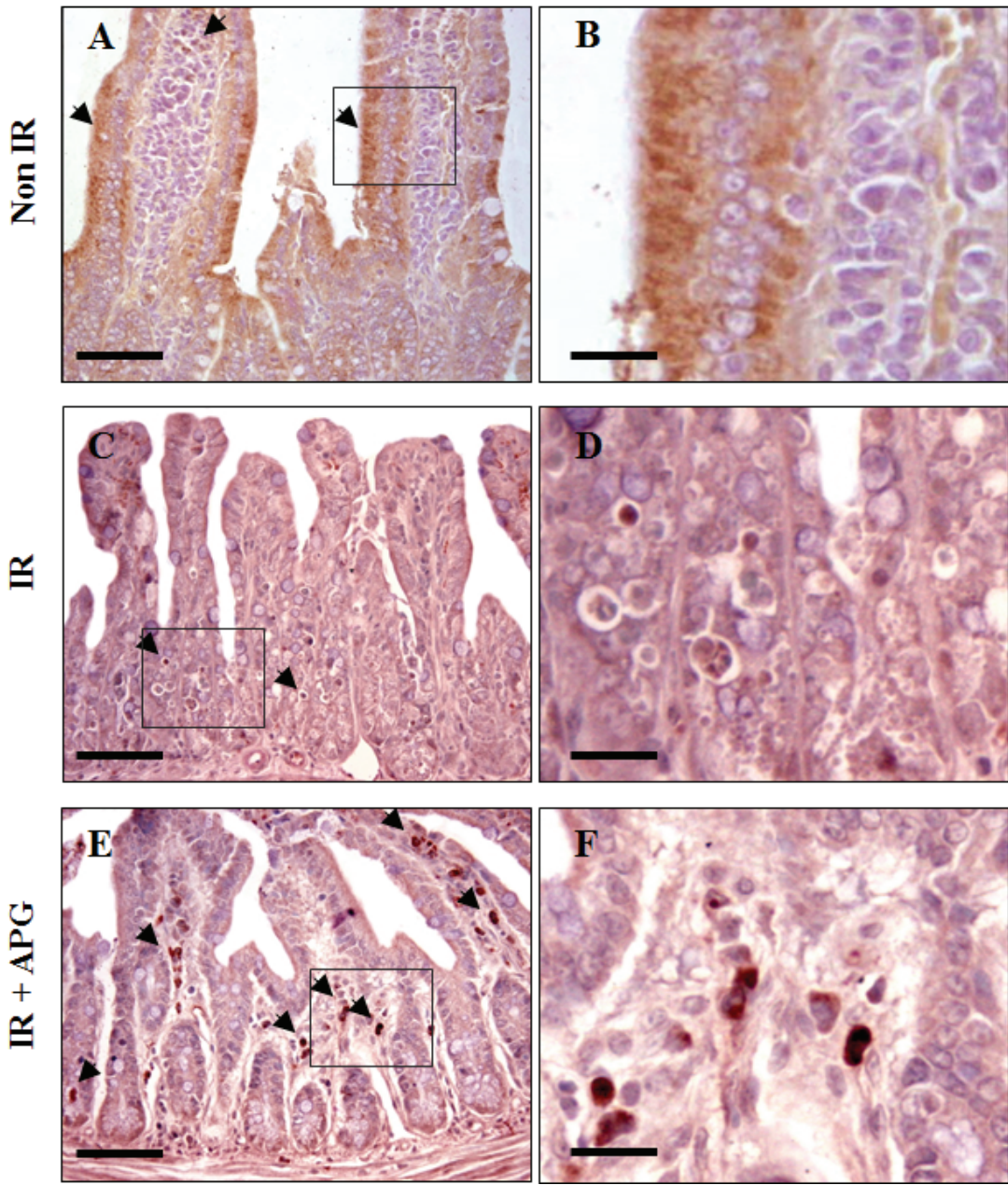


Figure 7. Bax immunoreactivity in small intestines of mice 24h after γ -ray irradiation. (A, B) Non irradiated-control, (C, D) Irradiated control, (E, F) APG plus irradiated group, (G) semi-quantitative analysis of immunohistochemistry for Bax, (H) Quantitative analysis of immunohistochemistry for Bax, (A, C, E) Bars = 60 μ m, (B, D, F) Bars = 30 μ m. (*; $P < 0.05$). Cells were counted as described in Materials and Methods. Results represent average and S.E. value in each experimental group. Data are representative of three independent experiments.



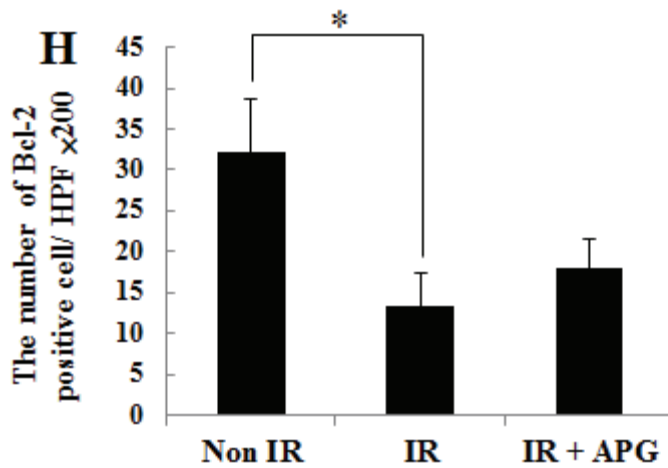
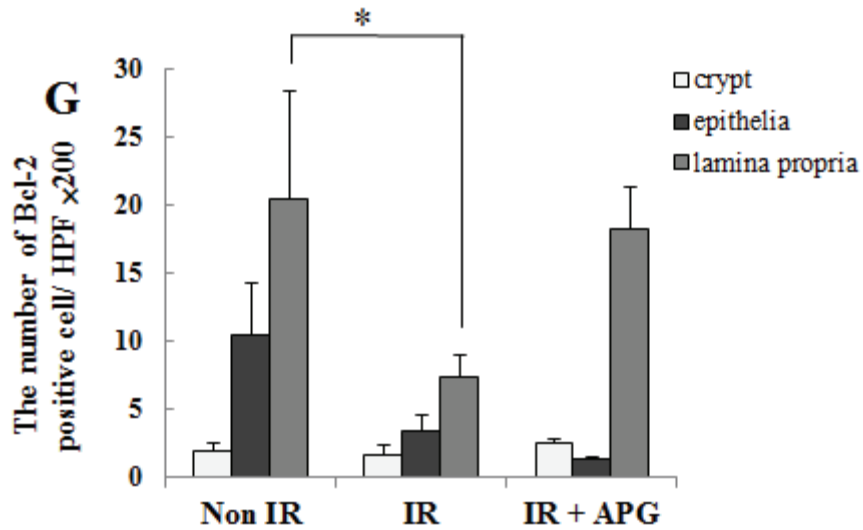
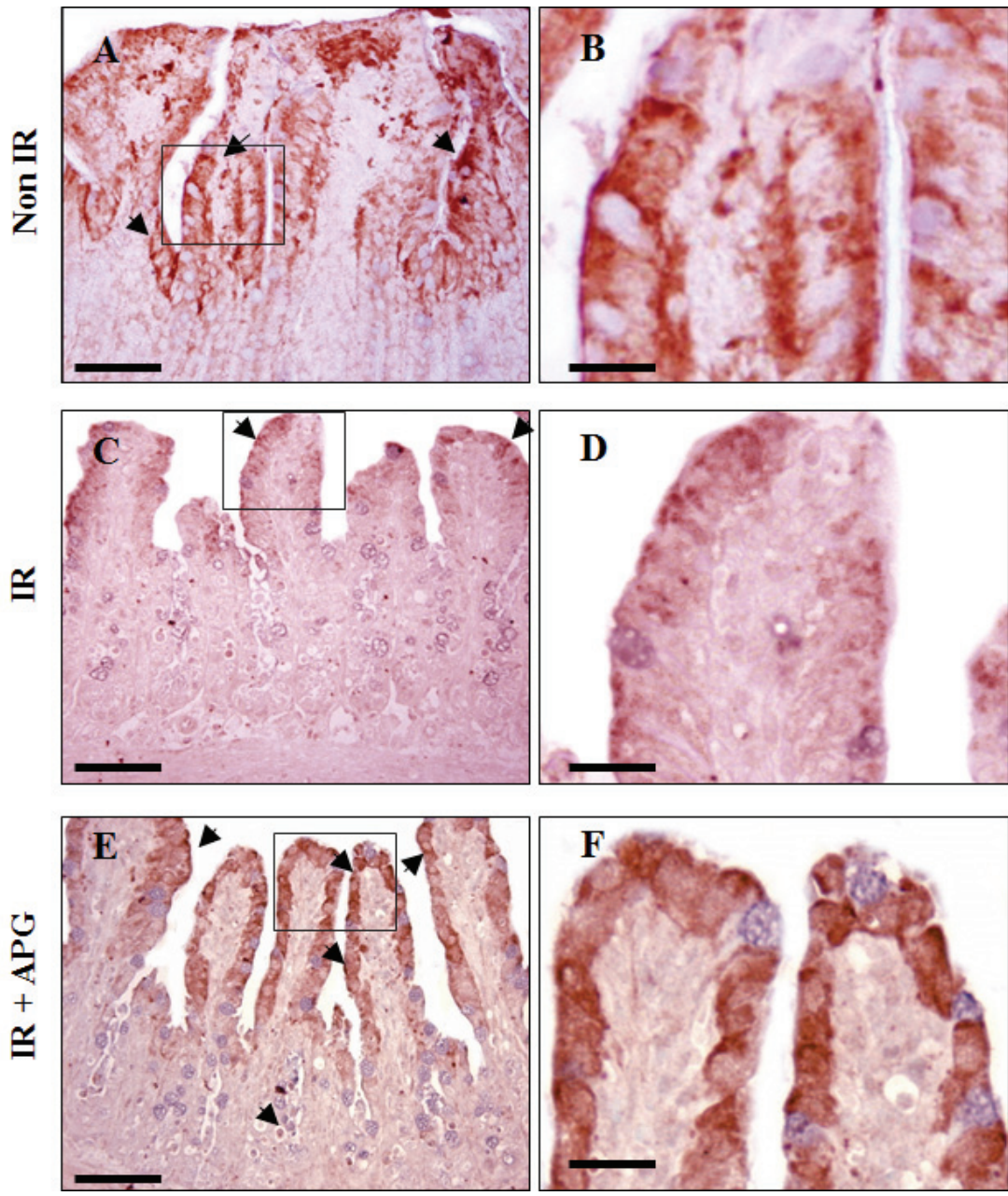


Figure 8. Bcl-2 immunoreactivity in small intestines of mice 24h after γ -ray irradiation. (A, B) Non irradiated-control, (C, D) Irradiated control, (E, F) APG plus irradiated group, (G) semi-quantitative analysis of immunohistochemistry for Bcl-2, (H) Quantitative analysis of immunohistochemistry for Bcl-2, (A, C, E) Bars = 60 μ m, (B, D, F) Bars = 30 μ m. (*; $P < 0.05$). Cells were counted as described in Materials and Methods. Results represent average and S.E. value in each experimental group. Data are representative of three independent experiments.



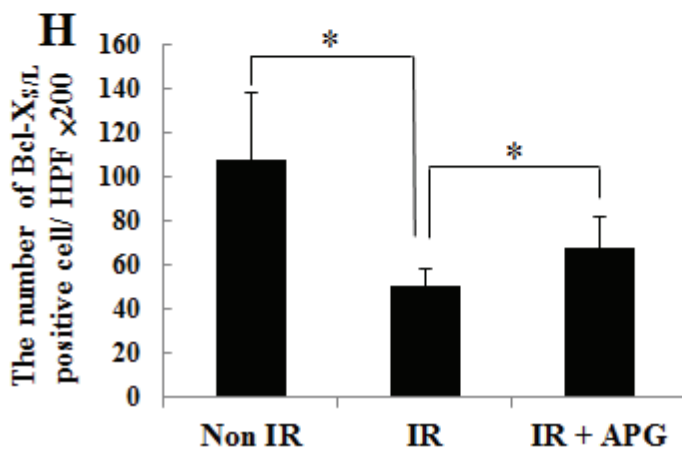
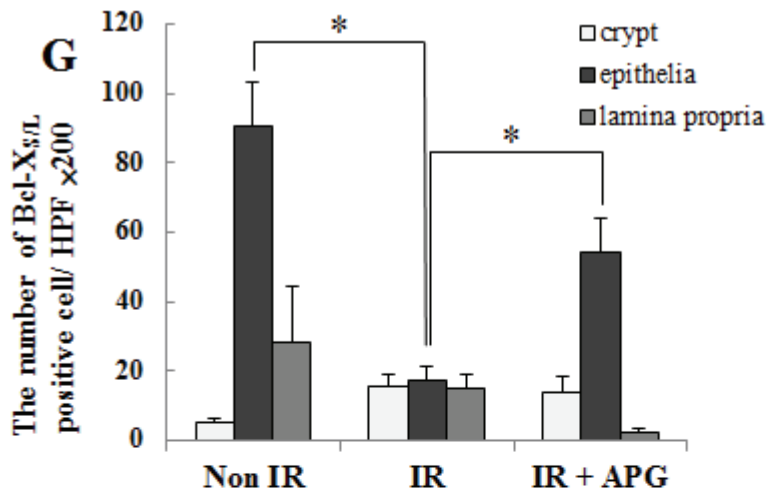
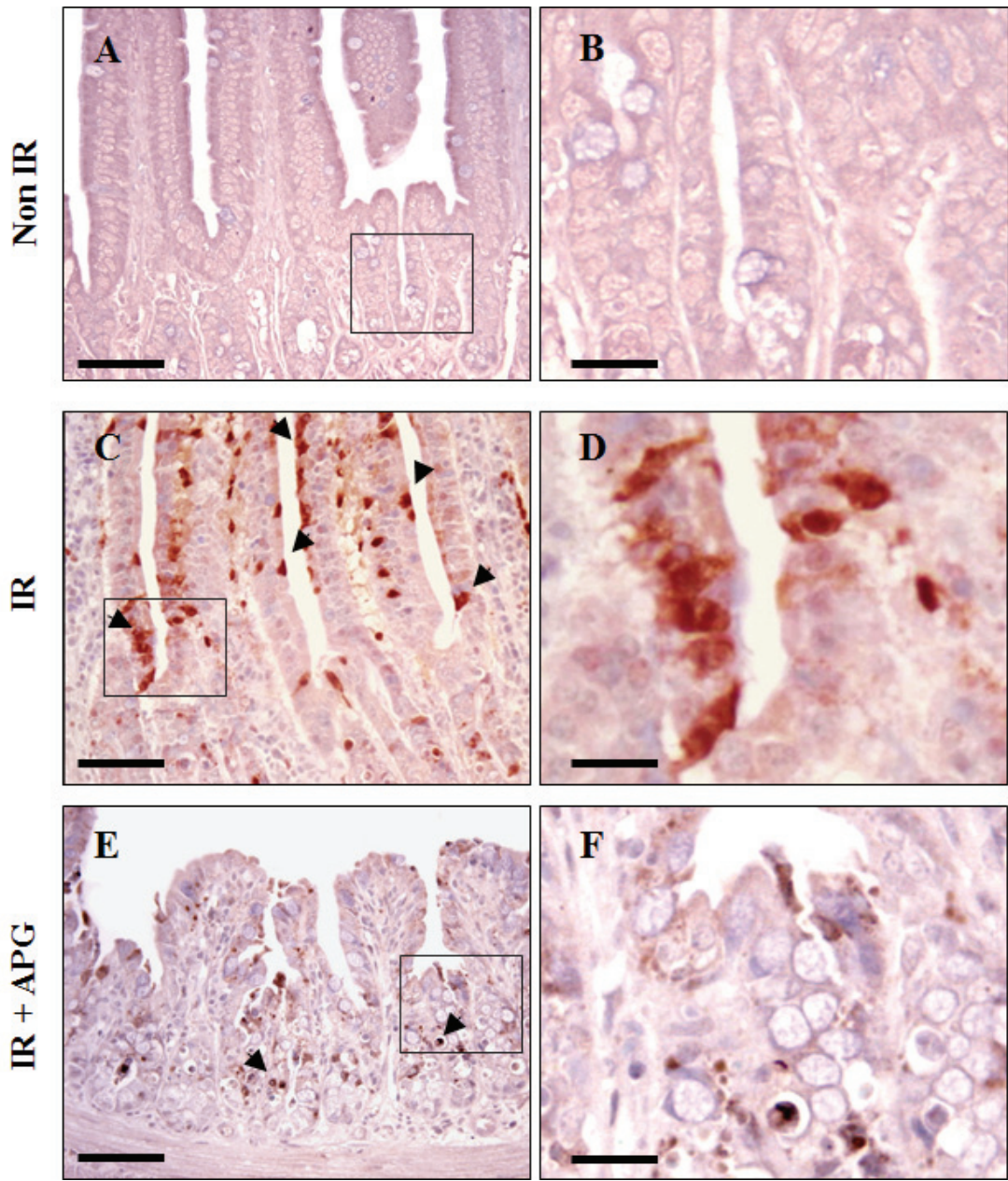


Figure 9. Bcl- $X_{S/L}$ immunoreactivity in small intestines of mice 24h after γ -ray irradiation. (A, B) Non irradiated-control, (C, D) Irradiated control, (E, F) APG plus irradiated group, (G) semi-quantitative analysis of immunohistochemistry for Bcl- $X_{S/L}$, (H) Quantitative analysis of immunohistochemistry for Bcl- $X_{S/L}$, (A, C, E) Bars = 60 μ m, (B, D, F) Bars = 30 μ m. (*; $P < 0.05$). Cells were counted as described in Materials and Methods. Results represent average and S.E. value in each experimental group. Data are representative of three independent experiments.



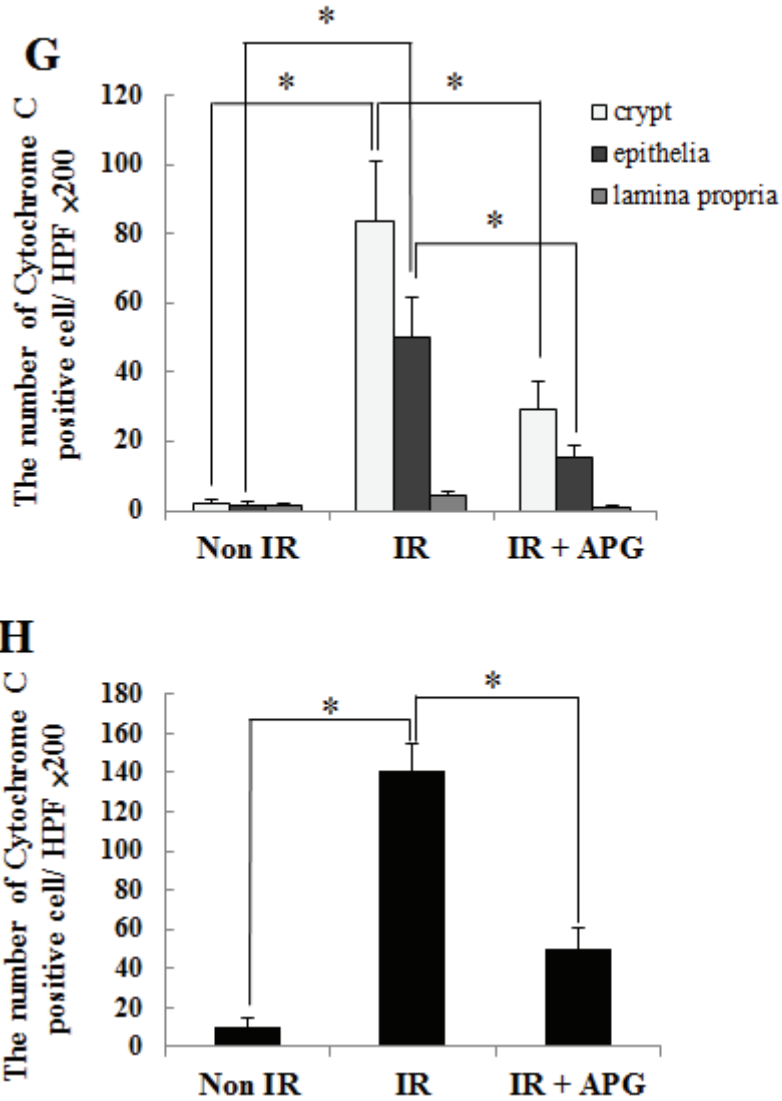
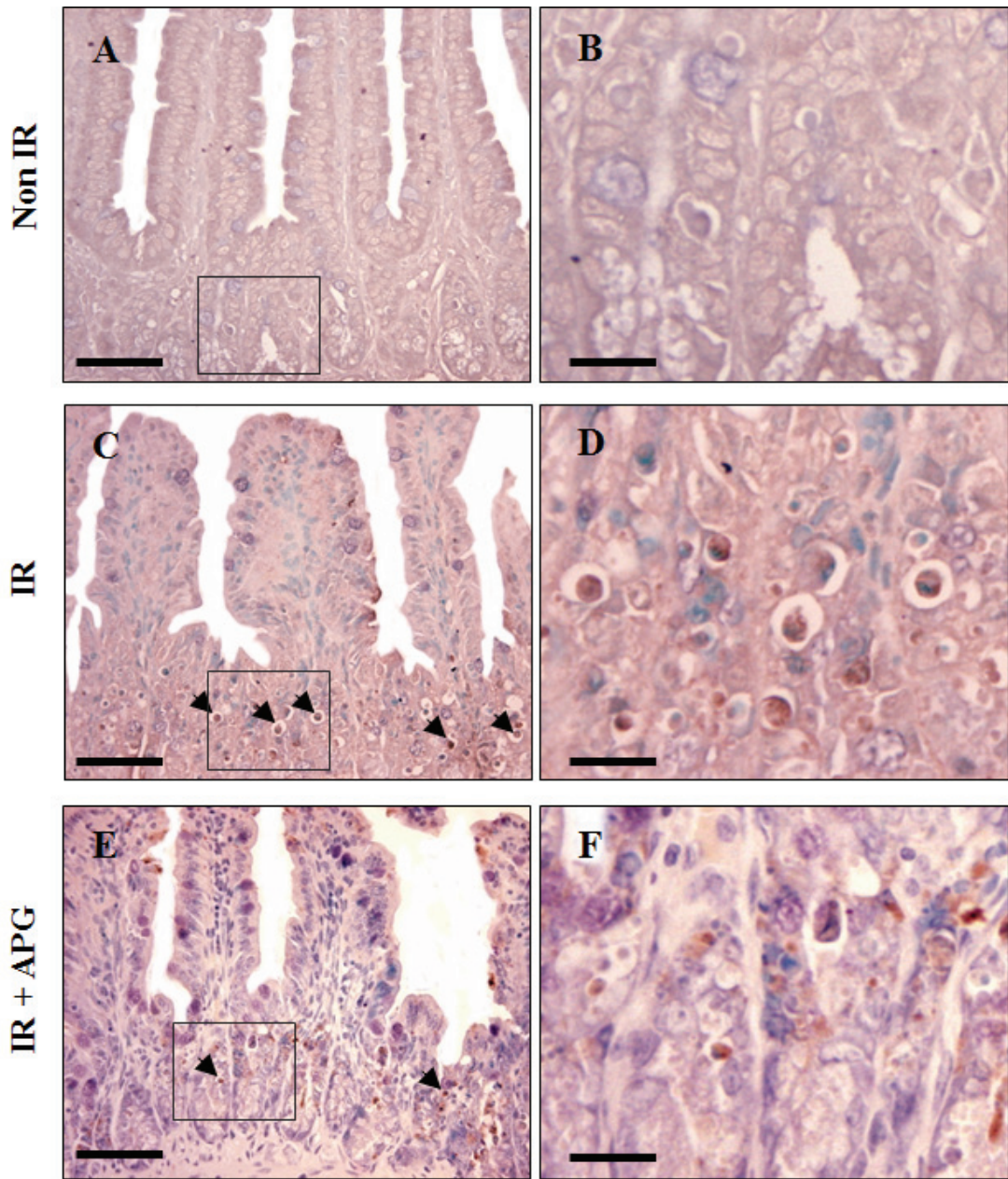


Figure 10. Cytochrome C immunoreactivity in small intestines of mice 24h after γ -ray irradiation. (A, B) Non irradiated-control, (C, D) Irradiated control, (E, F) APG plus irradiated group, (G) semi-quantitative analysis of immunohistochemistry for Cytochrome C, (H) Quantitative analysis of immunohistochemistry for Cytochrome C, (A, C, E) Bars = 60 μ m, (B, D, F) Bars = 30 μ m. (*; $P < 0.05$). Cells were counted as described in Materials and Methods. Results represent average and S.E. value in each experimental group. Data are representative of three independent experiments.



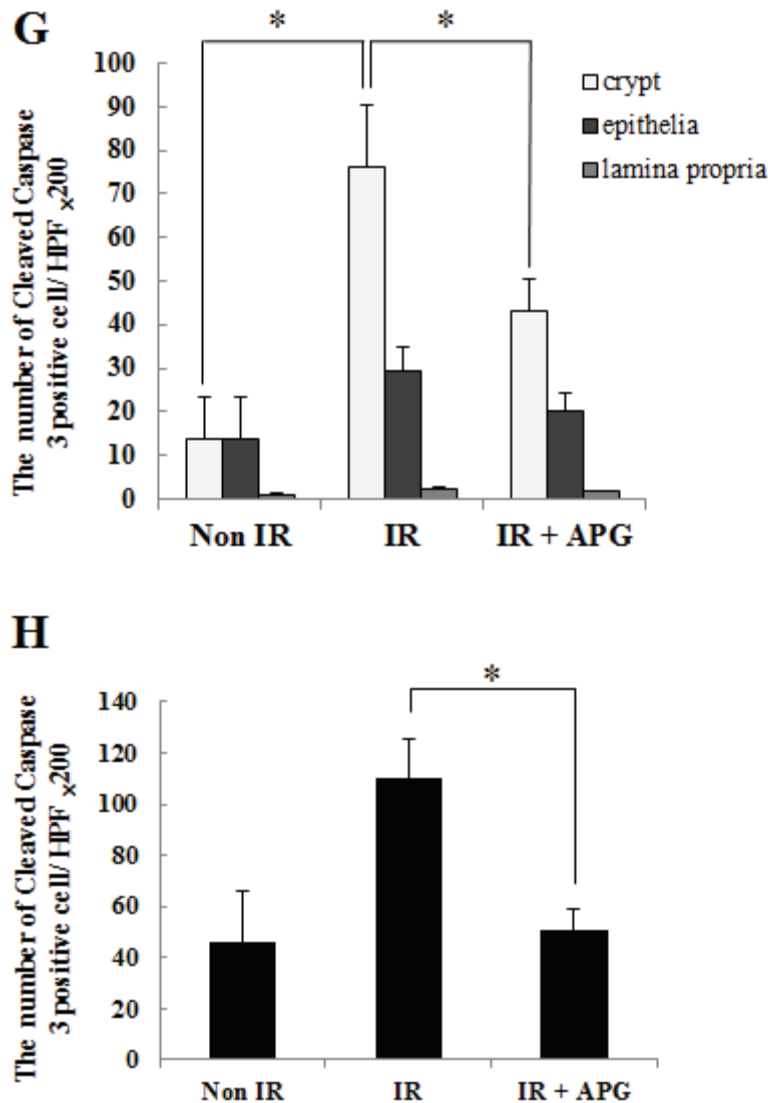


Figure 11. Cleaved caspase-3 immunoreactivity in small intestines of mice 24h after γ -ray irradiation. (A, B) Non irradiated-control, (C, D) Irradiated control, (E, F) APG plus irradiated group, (G) semi-quantitative analysis of immunohistochemistry for cleaved caspase-3, (H) Quantitative analysis of immunohistochemistry for cleaved caspase-3, (A, C, E) Bars = 60 μ m, (B, D, F) Bars = 30 μ m. (*; $P < 0.05$). Cells were counted as described in Materials and Methods. Results represent average and S.E. value in each experimental group. Data are representative of three independent experiments.

감마선 조사 마우스의 조혈 및 위장장애에 대한 인삼 acidic polysaccharide(APG)의 방어효과

지도교수 : 지영혼

김 대 승

제주대학교 대학원 수의학과

인삼 (panax ginseng)은 예로부터 건강식품 및 각종 생리활성 물질로 각광 받아 왔다. 흔히 인삼의 효능이라고 밝혀진 많은 결과들은 인삼의 구성성분인 사포닌 계열의 물질에 초점을 두어 밝혀진 것들이 많다. 하지만 최근 들어 항암, 항염, 항산화 등 중요한 효능을 가지고 있는 비사포닌 계열의 물질들 역시 많이 연구되고 있다. 그 중 acidic polysaccharide (APG) 역시 비사포닌 계열의 물질로서 암세포 살해세포 생성작용, 대식세포에 대한 면역조절자극 효과, 항균, 항염증 및 면역 조절 작용 효능에 관한 연구가 알려져 있다. 또한 APG의 방사선에 대한 방어제로서의 역할과 효능 연구로서 시험관내 실험에서 골수세포 방어작용, 항산화 작용에 의한 방사선 방호효과 등에 관한 연구가 진행되어 왔다. 따라서 본 연구에서는 마우스에서 방사선 손상에 대한 조혈 및 위장장애에 대한 APG의 방어효과를 알아보고 자세한 기전에 대해 확인하고자 하였다.

그 결과, 내재성 비장집락 형성시험을 통해 APG 병행투여군에서 내재성 비장집락 수의 증가를 확인할 수 있었고, Comet assay법을 이용하여 APG가 비장세포의 DNA손상을 효과적으로 억제 시킴으로서 말초면역 세포의 DNA손상 억제 효과가 있는 것을 확인할 수 있었다. 또한 DAPI 염색을 통해 비장세포에서 방사선 대조군에 비해 APG 병행투여군에서 apoptotic cell의 수가 유의적으로 감소하는 것을 관찰 할 수 있었다. 게다가 비장세포의 증식능시험에서 역시 방사선 대조군에 비해 APG 병행투여군에서 높은 수치를 나타내었다. 이후 소장 crypt에서 H&E염색 과 TUNNEL assay 염색을 통해 apoptotic cell의 수를 확인한 결과, 방사선 대조군

에 비해 APG 병행투여군에서 그 수가 유의적으로 감소하는 것을 확인할 수 있었다. 추가적으로 소장에서 세포자멸사 (apoptosis)와 관련된 인자들을 면역조직화학 염색법을 통해 발현양상을 알아보았다. 그 결과, anti-apoptotic 인자인 Bcl-2 와 Bcl-X_{S/L}은 방사선 대조군에 비해 APG 병행투여군에서 발현양상이 증가하였고, pro-apoptotic 인자인 p53, Bax, Cytochrome C, Caspase-3는 방사선 대조군에 비해 APG 병행투여군에서 발현양상이 감소하는 경향을 보였다.

결론적으로, 본 연구에서는 마우스에 방사선을 조사한 후 방사선 손상에 따른 조혈 및 위장장애에 대한 APG의 방호효과를 밝힘에 따라 APG는 방사선 방어물질로서 적용이 가능할 것으로 사료된다.

주요어 : 인삼 *acidic polysaccharid (APG)*, 감마선, 조혈 및 위장장애, 세포자멸사 (*Apoptosis*)